ARL 65-260
DECEMBER 1965

Aerospace Research Laboratories

ADVANTAGES OF A 4-AXIS TRACKING MOUNT FOR THE PHOTOELECTRIC PHOTOMETRY OF SPACE VEHICLES

KENNETH E. KISSELL
GENERAL PHYSICS RESEARCH LABORATORY

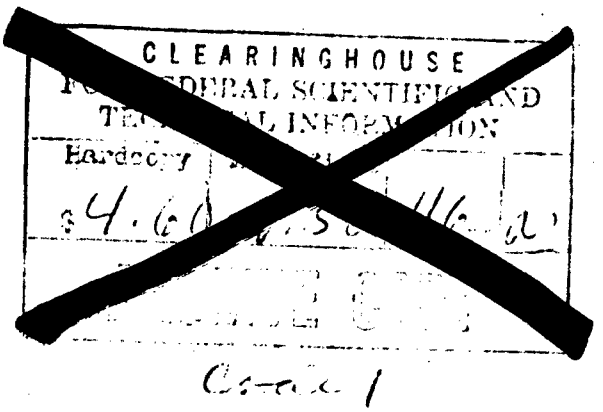

Copy 1

OFFICE OF AEROSPACE RESEARCH
United States Air Force

ARL 65-260

ADVANTAGES OF A 4-AXIS TRACKING MOUNT FOR THE PHOTOELECTRIC PHOTOMETRY OF SPACE VEHICLES

KENNETH E. KISSELL

GENERAL PHYSICS RESEARCH LABORATORY

DECEMBER 1965

Project 7114

AEROSPACE RESEARCH LABORATORIES
OFFICE OF AEROSPACE RESEARCH
UNITED STATES AIR FORCE
WRIGHT-PATTERSON AIR FORCE BASE, OHIO

FOREWORD

This report summarizes the experience and analysis leading to the desi and construction of a 24-inch aperture, 4-axis satellite tracking telescope n in constant use at the Aerospace Research Laboratories Sulphur Grove Fiel Site some six miles north of Dayton, Ohio. The work detail herein was con· ducted in 1960 to 1963 under various research tasks at ARL. This work is now pursued under the Research Task, "Photoelectric Photometry of Space Vehicles", Project 7114.

This paper was presented to the COSPAR Working Group 1, at the Fifth International Space Science Symposium in May 1964. It is now published as AF Technical Report since only an abstract was published in Space Researcl p. 915, North-Holland Publishing Co., Amsterdam (1965) and since the cont of this paper is fundamental to more recent developments in satellite trackir and satellite signature research.

ABSTRACT

Arguments are presented for the necessity of using a four-axis telescope (Quad-R-Axial) mount for the photoelectric photometry of satellites if small field apertures and hence low sky background signals are to be achieved. Since the signal to noise ratio of the target/ background is proportional to the square of the diameter of accepted field, any reduction of guiding errors which will allow smaller field apertures will then allow the photometry of fainter satellites, providing telescopes of adequate aperture are used. The improved tracking will also reduce interruptions of the light curves resulting from loss of the vehicle from the sensing aperture. The improvements possible with a QRA mount over the 2-axis (alt-azimuth) and the 3-axis (Baker-Nunn) are shown and procedures for computation of mount settings established. Photoelectric data taken with an existing 3-axis system are given for several satellites.

TABLE OF CONTENTS

LIST OF ILLUSTRATIONS

INTRODUCTION

Up to the present time, studies of space vehicles by optical means have been almost entirely limited to astrometry. The geodetic and geophysical sciences have utilized time/position data for studies of oblateness, mass asymmetry, and outer atmospheric density. The utilization of the time-dependent brightness changes of space vehicles has lagged behind, almost analogous to the situation in stellar astronomy where astrometric catalogues of star positions were made decades before systematic photometric measurements were begun. Approximately a dozen references are available either suggesting or utilizing the photometric properties of satellites. A synopsis [1-13] of these is given in Appendix A. The most significant of these are the studies by NOTS[5,6] of the ozone absorption utilizing 1960 ι 1, the early USSR work by visual photometry[1,2] on the rigid-body rotation of 1957 β 1 and 1958 δ 1, utilization by Bell Telephone Laboratories[7,8,9] of coded flashes from 1962 α ϵ 1 for spin-axis determination, and the Smithsonian Astrophysical Observatory[10,11] analysis of spatial position of flash maxima in terms of vehicle orientation. Utilizing the precision of photoelectric photometry, the author, in conjunction with others[13] has undertaken extension of the USSR work and the interpretation of the detailed shape of the light curves. The success of this work has led to the present study of tracking mounts in an effort to improve the quality of the light curves and to ease the difficulties of tracking.

The use of photometric data in the determination of spin-axis and vehicle-axis orientation requires data on successive transits or on successive days, i.e. data taken from differing positions with respect to the vehicle-centered inertial reference frame. For low-altitude satellites this normally requires tracking of vehicles at large zenith distances. Even for high satellites data at large zenith distances are necessary to obtain maximum divergence of observer/vehicle vectors, although these data could perhaps be obtained at low elevation of near-zenith transits. Before considering the possible advantages of a more flexible telescope mounting for improved tracking at large zenith distances, it is appropriate to ask whether one might expect a large number of near-zenith transits for a satellite at any given topocentric height, i.e. are the requirements for photometric study met by the frequency of transits with small zenith distances?

PROBABILITY OF SATELLITE TRANSIT AT ZENITH DISTANCE LESS THAN Z

For a simple case consider a satellite in a circular orbit of high inclination, polar for illustration. For a station located on the equator, there is equal probability, a priori, that during some transit the station will lie at any specified longitudinal distance from the ascending nodal crossing of the satellite, up to a distance of one-half of the nodal separation due to rotation of the earth between two consecutive orbits. That is to say that it is equally likely that the satellite will cross the equator east or west of the observer at any point up to one-half of a nodal separation. If the equatorial crossing point just exceeds one-half the nodal separation on a given revolution, it will lie less than a half separation on the next revolution. Referring to Figure 1, and defining Γ as the half-separation of the nodes one can express the probability as

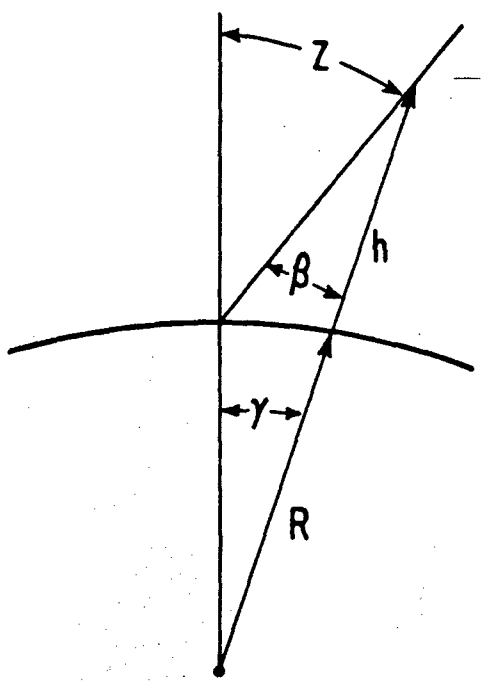

GREAT CIRCLE DISTANCE TO A SATELLITE AT ZENITH DISTANCE, Z, AND TOPOCENTRIC HEIGHT, h.

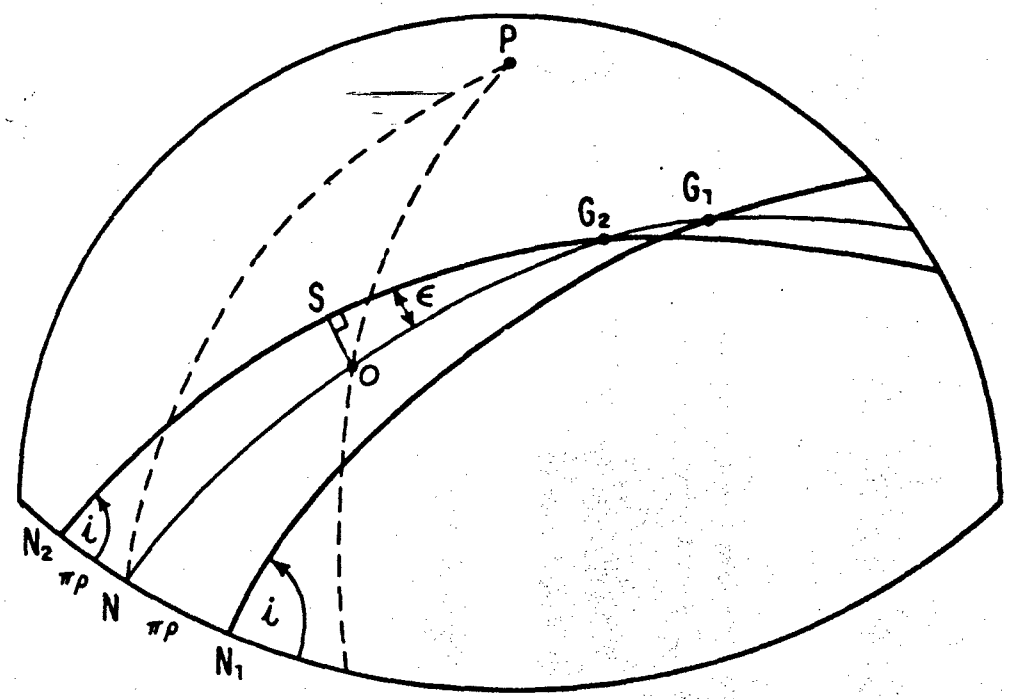

GEOMETRIC CONSTRUCTION FOR SOLUTION OF GREAT CIRCLE DISTANCE TO SUB-SATELLITE POINT FROM AN OBSERVER MIDWAY BETWEEN SUCCESSIVE TRANSITS.

Figure 1

Geometry of the Visibility of a Satellite at Height h in an Orbit of Inclination i

$$\bar{P} = \frac{\gamma}{\Gamma} = \frac{\pi - \beta - (\pi - Z)}{p\pi} = \frac{Z - \beta}{p\pi}$$

Here γ is the geocentric angle subtended by the great circle arc connecting the observer and sub-satellite point for the satellite at the smallest zenith distance Z, β is the complement of the depression angle of the observer as seen from the satellite, and p is the nodal period of the satellite in sidereal days. If the observer is not at the equator but at a latitude ϕ, this equation must be modified to account for the convergence of the orbital trajectories toward the poles.

The probability for polar orbits and a station at latitude ϕ may be expressed as

$$\bar{P} = \frac{Z - \beta}{\text{arc sin}\,(\sin \pi p \cdot \cos \phi)}$$

For the more general case of observation of satellites in circular orbits of inclination i from a station at latitude ϕ somewhat less than i, one can solve for the great circle distance to the sub-satellite point S from the observer at point 0 with the aid of Figure 1b, where arc 0S is the great circle normal to the sub-satellite trajectory N_2SG.

In Figure 1b the arcs N_1G_1 and N_2SG_2 represent sub-satellite traces of successive orbits of the satellite. These traces are then separated at the nodes by $N_1N_2 = 2\pi p$. Arc NOG_2G_1 is the great circle of inclination i crossing the equatorial plane midway between N_1 and N_2 and approximately represents the trace of observer locations midway between transits. The arc length OS corresponds to half separation Γ of the nodes for the equatorial case above. Calling this Γ^1

$$OS = \Gamma^1 = \text{arc sin}\,(\sin \epsilon \cdot \sin 0G)$$

where

$$\epsilon = \text{arc cos}\,(\cos^2 i + \sin^2 i \cdot \cos \pi p)$$

$$OG = NG - NO = NG - \text{arc sin}\,(\sin \phi / \sin i)$$

$$NG = \text{arc sin}\,(\sin \pi p \cdot \sin i / \sin \epsilon)$$

The a priori probability of a transit within a zenith distance Z is then

$$\bar{P} = \frac{Z - \sin^{-1}\left(\frac{1}{1+h}\right)\sin(\pi - Z)}{\sin^{-1}\left(\sin\left[\cos^2 i + \sin^2 i \cos \pi p\right]\right)} \quad ----$$

$$---\times \sin\left[\sin^{-1}\left(\frac{\sin \pi p \times \sin i}{\sin\left\{\cos^{-1}\left[\cos^2 i + \sin^2 i \cos \pi p\right]\right\}}\right) - \sin^{-1}\left(\frac{\sin \phi}{\sin i}\right)\right]$$

where

$$\beta = \text{arc sin}\left[\frac{R}{R+H}\sin(\pi - Z)\right]$$

$$P = \sqrt{k}\left(\frac{R+H}{R}\right)^{3/2} \qquad \text{sidereal days}$$

where R is the earth radius, H the satellite height above the surface, and k the Gaussian Constant = 3.4630×10^{-3} day^2 Earth Radii^{-3}

The dependence of near-zenith probability on satellite height is given in Figure 2 for a station at 40° latitude and zenith distances of 30° and 45°. It is apparent that the probability is low for near-zenith transits of polar satellites a heights less than 600 kilometers and in fact does not approach unity at any heig for zenith distances less than 40°. This is the result of the diverging nodal separation for satellites of longer and longer periods. While the result is modified for lower inclinations of the orbit plane, the example chosen clearly illustrates that photometric observations or observation by long-focus cameras from fixed stations will probably be done at large zenith distances unless the inclination of the satellite corresponds nearly to the latitude of the observing station. Figure 3 illustrates the expectation of transits within 30° of the zenith for various station latitudes for a satellite in an orbit of 65° inclination. Thus, except for coincidental circumstances when the satellite period brings the vehicle over the same geographical region for several successive days, one cannot expect to obtain near-zenith transits on frequent occasions. Photoelectric photometry of satellites must therefore be conducted at large zenith distances.

Under the conditions of large zenith distance of culmination, the tracking c the satellite by alt-azimuth, equatorial, or triaxially-mounted telescopes becomes difficult. Extinction corrections become quite important in photometry as well as variable sky background; in fact, all of the common hazards of stellar photometry are present. This paper is directed to the problem of

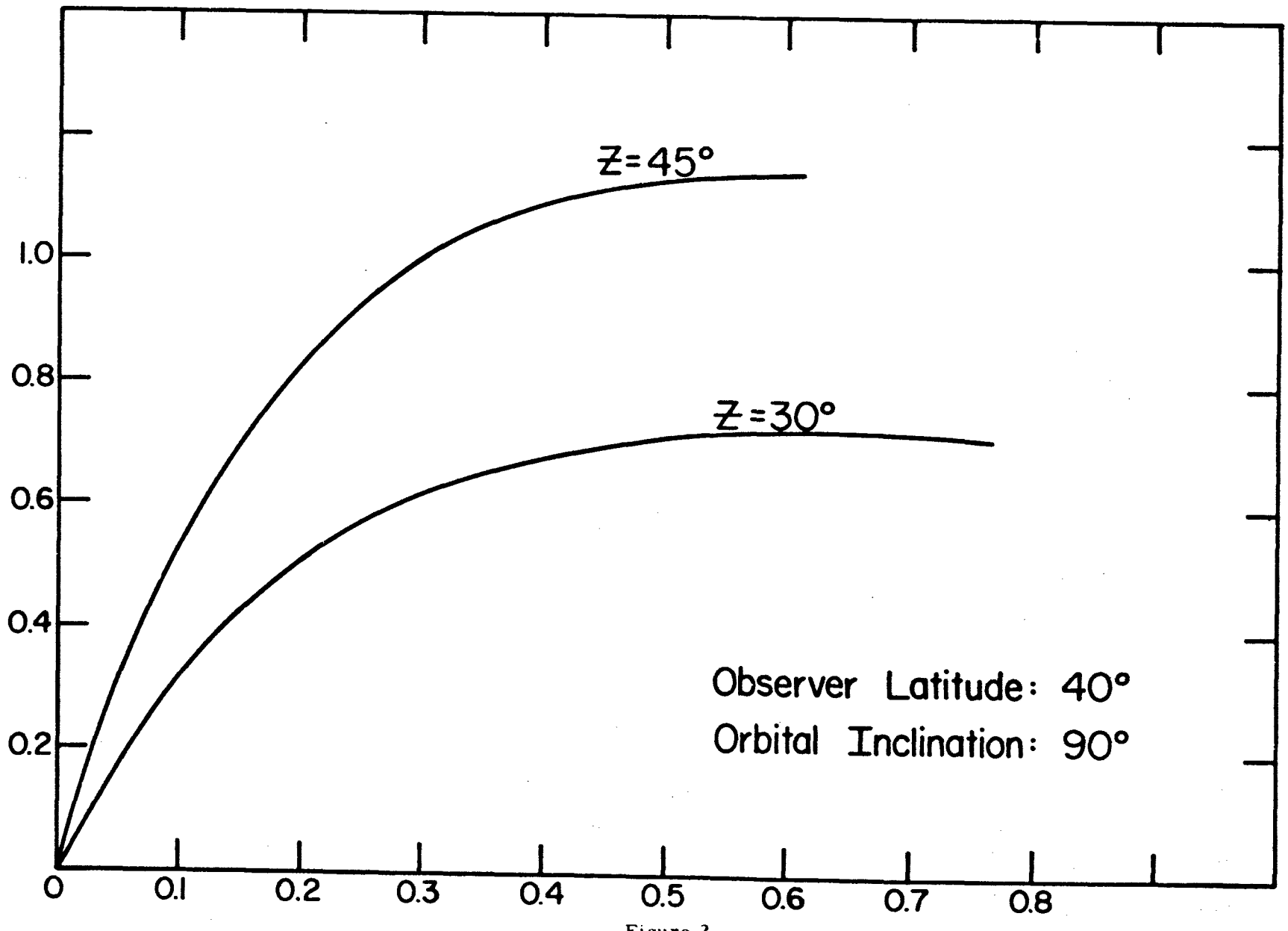

Figure 2

Probability of daily occurrence of transits at zenith distances less than Z for polar satellite, observer at Latitude 40°.

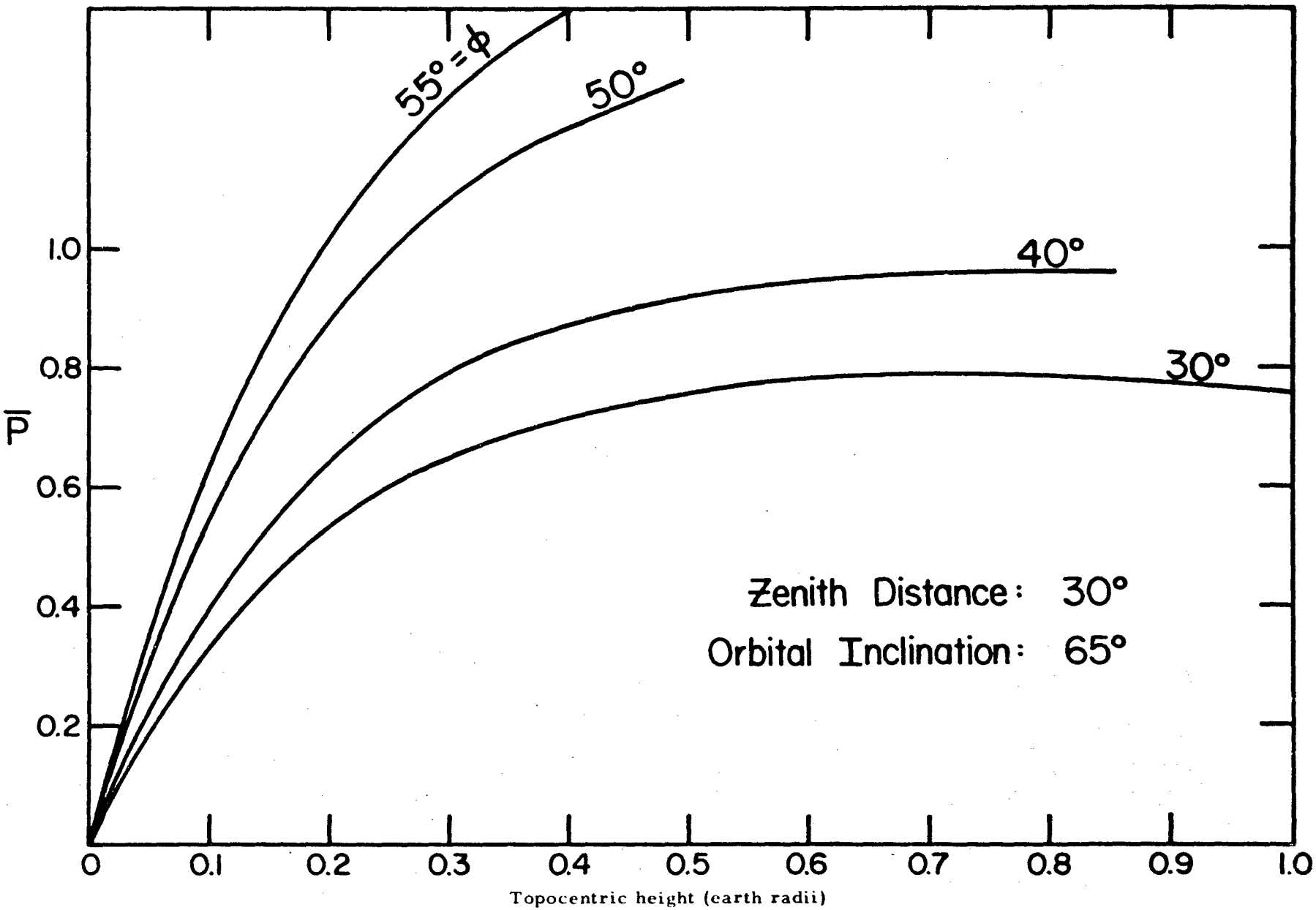
55° = φ
50°
40°
30°
1.0
0.8
0.6
0.4
0.2
$\overline{P}$
Zenith Distance: 30°
Orbital Inclination: 65°
0
0.1
0.2
0.3
0.4
0.5
0.6
0.7
0.8
0.9
1.0
Topocentric height (earth radii)

Figure 3

narrow-field tracking to improve the continuity of data and to reduce the sky background signal by allowing use of small field apertures.

GREAT CIRCLE APPROXIMATION

In 1955 the Smithsonian Astrophysical Observatory undertook the optical tracking of the IGY satellites. It was early realized that the photographic recording of the Vanguard vehicles would be impossible using fixed cameras inasmuch as the exposure time would be limited to the time required for the diffraction image to translate an emulsion resolution element in the focal plane. The three-axis Baker-Nunn camera was perfected as the solution for providing a means of reducing the satellite's apparent velocity to a value near zero with respect to the emulsion. As shown in Figure 4, the 3-axis system closely approximates the satellite's motion at one or two points during the satellite transit by moving the camera on a great circle path tangent to the apparent trajectory. It is apparent that, except at the culmination point, there remains a component of motion normal to the camera motion. It is either this cross-track motion of the image or a slight mismatch of the tracking rate which represents the ultimate limit in exposure time. An error of one percent in the matching of velocity restricts the gain of the 3-axis mount over a fixed camera to 5 stellar magnitudes[14] (from magnitude 8.5 to 13.5 for satellites at rates of 0.1 degrees per second, i.e. ranges of 4000 to 4500 km).

Since the orbital elements of the satellite and hence its actual path across the sky are imperfectly known, errors will exist in the pointing of the camera axes and in the camera angular velocity. These errors are of secondary importance in the case of satellite astrometry since the camera field of view is $5^{o} \times 30^{o}$ with the greater dimension in the direction of motion of the satellite. Depending on the height of the satellite and hence its apparent angular rate, an error of 15-150 seconds can be tolerated in the predicted time of culmination with recording of the satellite still assured on the frame. This results from the secondary dependence of the elevation angle of the satellite path on the actual time of culmination passage.

If one seeks to do photoelectric photometry, it is necessary to place the satellite image within a small entrance aperture at the focal plane of the telescope in order to reduce the sky background to tolerable levels. In the case of stellar photometry, the precise guiding of an equatorial mount allows use of apertures of a few seconds of arc apparent field; the aperture is chosen to assure capture of the entire diffraction disk of the star while allowing for seeing variations in the image position. The much larger and varying rate of a satellite target requires apertures measured in minutes of arc rather than seconds to assure capture of the vehicle during most of its transit. Experience with the satellite photometer now in use at the ARL Sulphur Grove Field Site has shown that apertures of 3-7 minutes of arc are tolerable with a 3-axis tracking system. The system, shown in Figure 5, consists of a Nunn mounting built by Boller & Chivens, Inc., a 12-inch catadioptric cinetheodolite objective of 60-inch focal length rigidly attached to the central steel plate which replaced the Baker-Nunn camera, and a photoelectric photometer.

The Graham transmission drive allows tracking in either direction at rates continuously variable from zero to 7200 seconds of arc per second in three speed

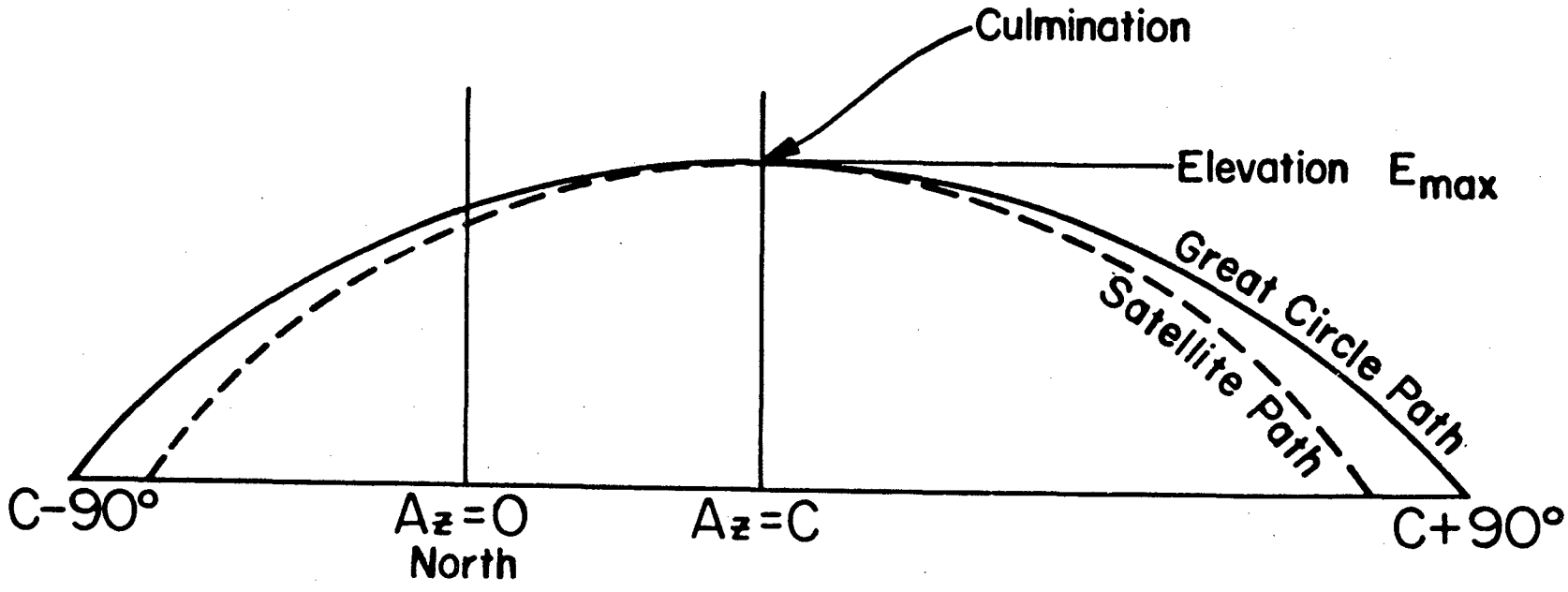

Figure 4

Great circle approximation to the apparent trajectory of a satellite.

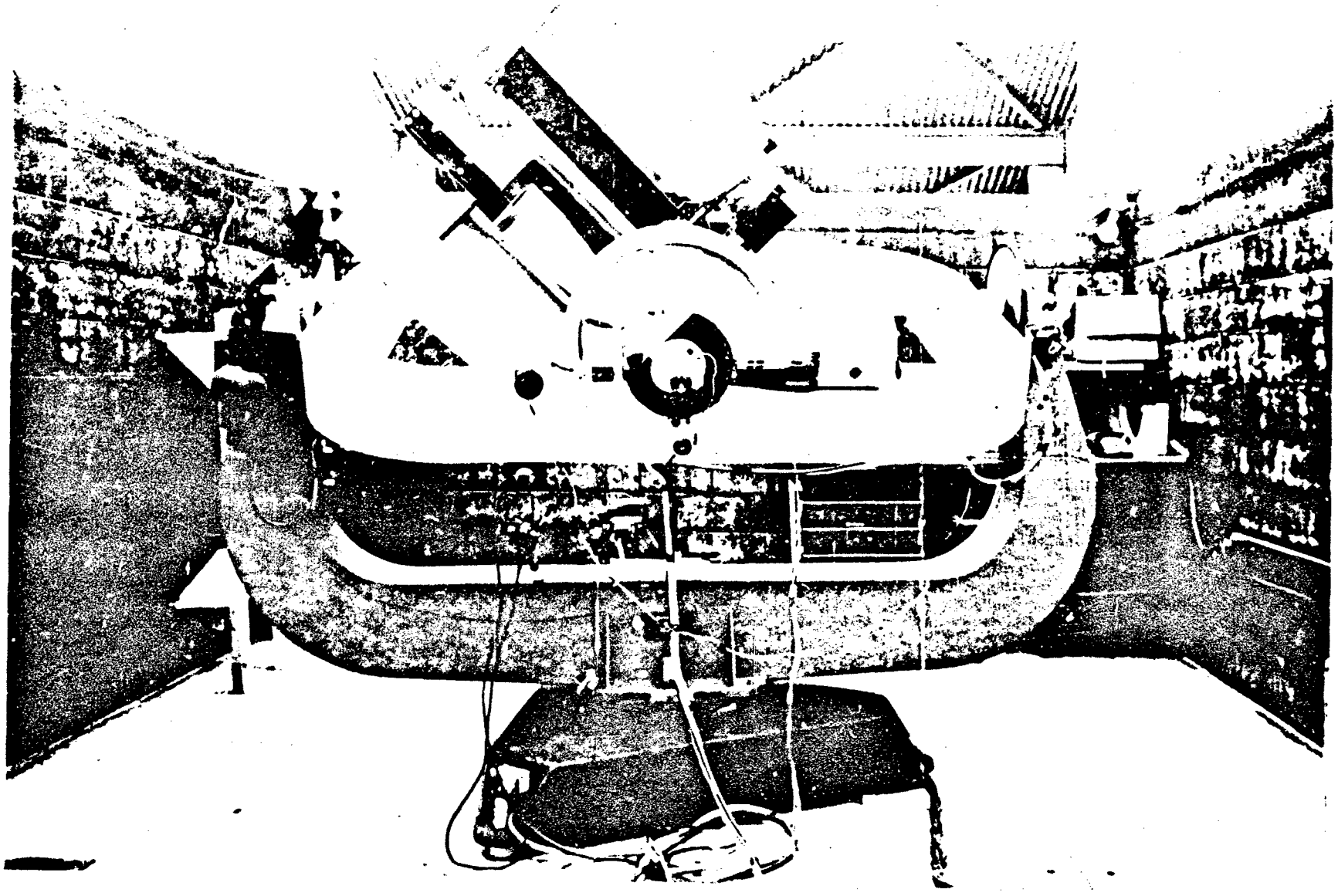

Figure 5

Tri-axial satellite photometer system

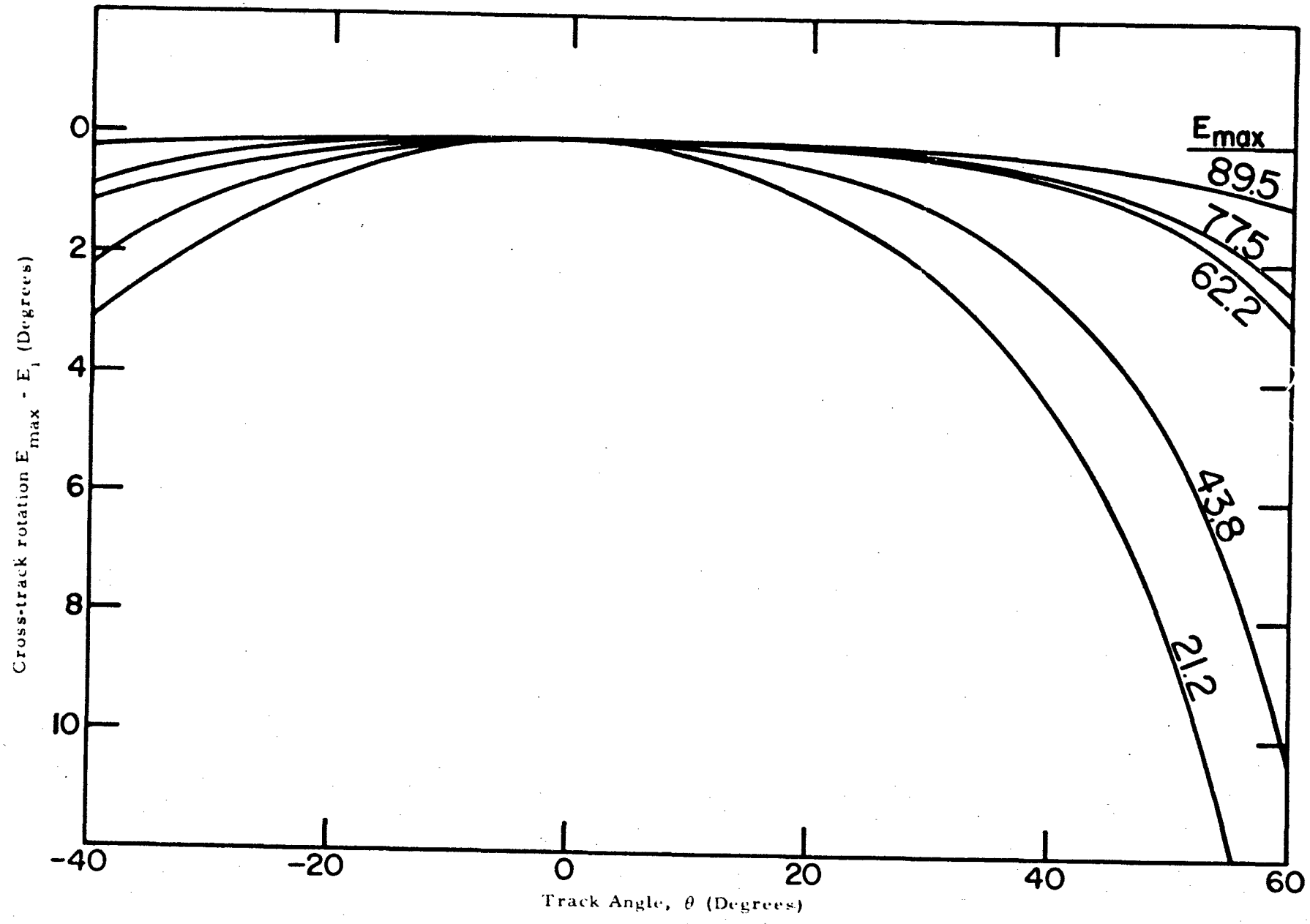
Emax
89.5
77.5
62.2
43.8
21.2
0
2
4
6
8
10
-40
-20
0
20
40
60
Cross-track rotation $E_{max} - E_1$ (Degrees)
Track Angle, θ (Degrees)

Figure 6

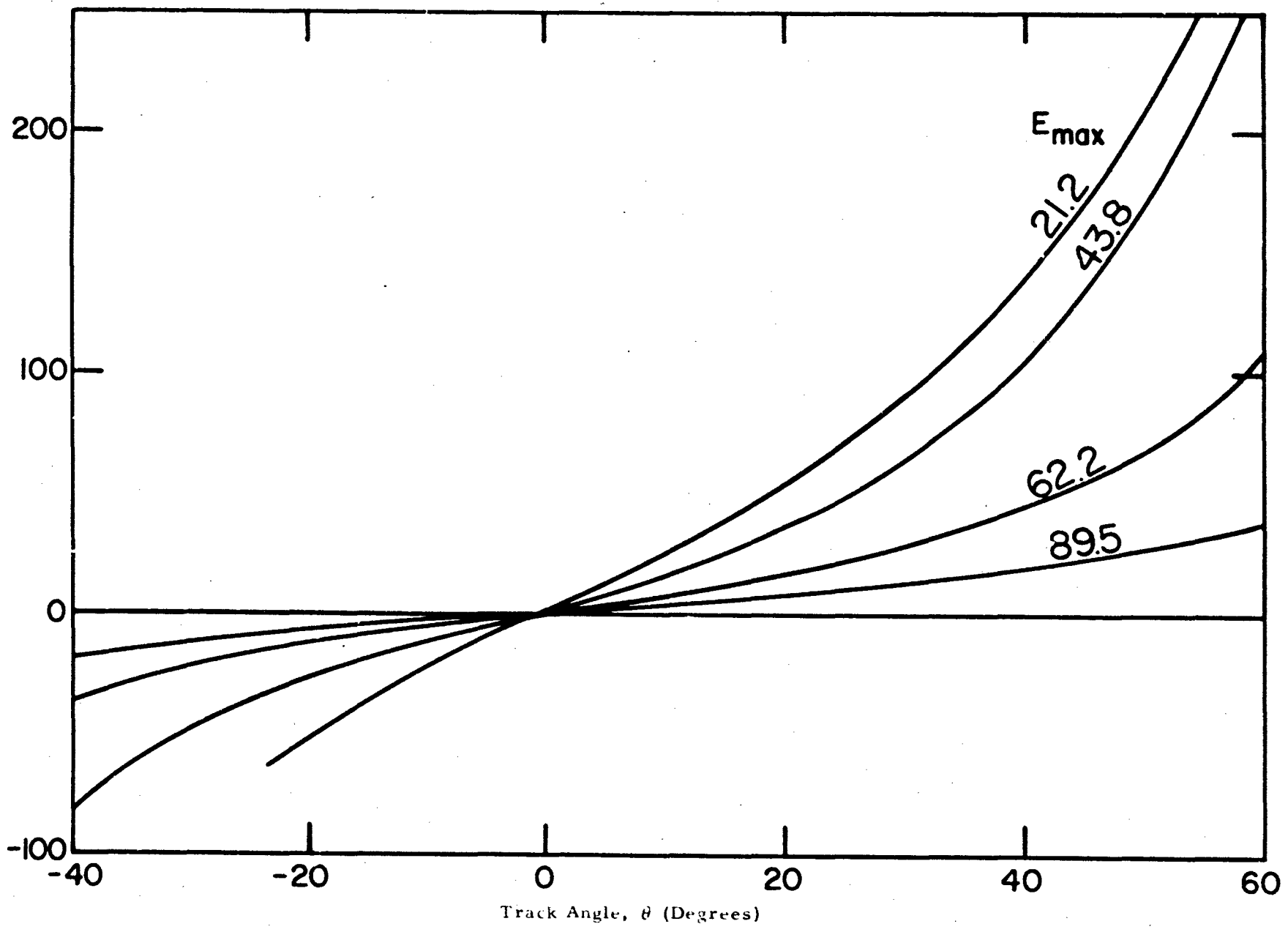

Figure 7

Cross track velocity as a function of track angle and elevation of culmination for satellite in near-circular orbit at height of 1000 kilometers, 1962 β α2.

ranges, 0-72, 0-720, and 0-7200, and a manually-controlled servo-motor permitted adjustment of the cross-track axis. Azimuthal adjustment is by hand and the azimuth axis is locked prior to the satellite transit. Shaft position digitizers permit the operator to read the tracking or cross-track angles to $\pm$0.1 degrees on a Nixie display without moving from the mount.

Acquisition and tracking of the satellite is visual and manual. The mount is positioned to predetermined angles at a favorable point along the predicted trajectory. The acquisition is enabled by a 20 x 125 elbow telescope (NRL/ SAO apogee telescope) with a 2.2 degree field of view. The active field of the photometer within the guider field is checked by bore sighting on a convenient star. The photoelectric photometer utilizes a feedback circuit for logarthmic response, i.e., output linear in stellar magnitude, described in more detail in Appendix B. The feedback signal also modulates an audio tone transmitted to the observer for verification of the successful tracking of the vehicle. From practical experience it is relatively easy to obtain continuous tracking of transits reaching culmination above 60 degrees elevation and relatively difficult for transits below 30 degrees. This latter difficulty results from the large amount of cross-track motion necessary to overcome the error in the great circle approximation. Figure 6 shows the variation of cross-track position with track angle for transit 89.5, 77.5, 62.2, 43.8, and 21.2 degrees culmination for a vehicle in a 1000 kilometer high orbit. Figure 7 shows the cross-track velocities for several of these same transits. It is apparent that the cross-track velocities increase markedly for low transits, seriously limiting the continuity and duration of photometric records. Figures 8, 9, and 10 show photometric records of a satellite exhibiting a combination specular and diffuse reflection, 1962 β α-2, and two satellites exhibiting a diffuse reflection, 1963-10B and 1962 β θ-2. Tracking rates on these vehicles were approximately 0.3 and 0.5 degrees per second. Figure 9 exhibits several instances of signal dropout as the result of cross-track or tracking rate errors.

EQUATION OF MOTION FOR QUAD-R-AXIAL MOUNT

One seeks to improve on the tracking accuracy of the tri-axial mount as applied to the earth satellite problem. It is observed that the beginning and end of the apparent trajectory of a satellite (as seen by a topocentric observer) drop below the great circle approximation given by the tri-axial mount, i.e. the rise and set points of the trajectory are less than 90° in azimuth from the azimuth of culmination, C, which is demonstrated in Figure 4. Reflection on this fact suggests that the path traversed by the satellite would be better approximated by a mount similar to an equatorial mount for a conventional telescope, where the telescope may deflect towards "Southern declination". This is suggested by the analogy to the motion of stars of southern declination which rise and set at azimuth less than 90° from the meridian. The advantages of such an additional axis were first pointed out to the author by H. F. A. Tschunko in 1959. M. Liigant and Ya. Einasto[15] analyzed the advantages of such a system for satellite tracking by servo-controlled telescopes. However, the system has not yet found acceptance in satellite astronomy. Figure 11 shows the geometry of such a system. Here the satellite is at position X on its path W X Y which reaches the maximum elevation E_{max}. To approximate this path with a quadraxial tracking telescope, one first makes an azimuthal adjustment to set the telescope polar axis into the plane of E_{max} Z. The polar axis is then adjusted in angle so that the equatorial

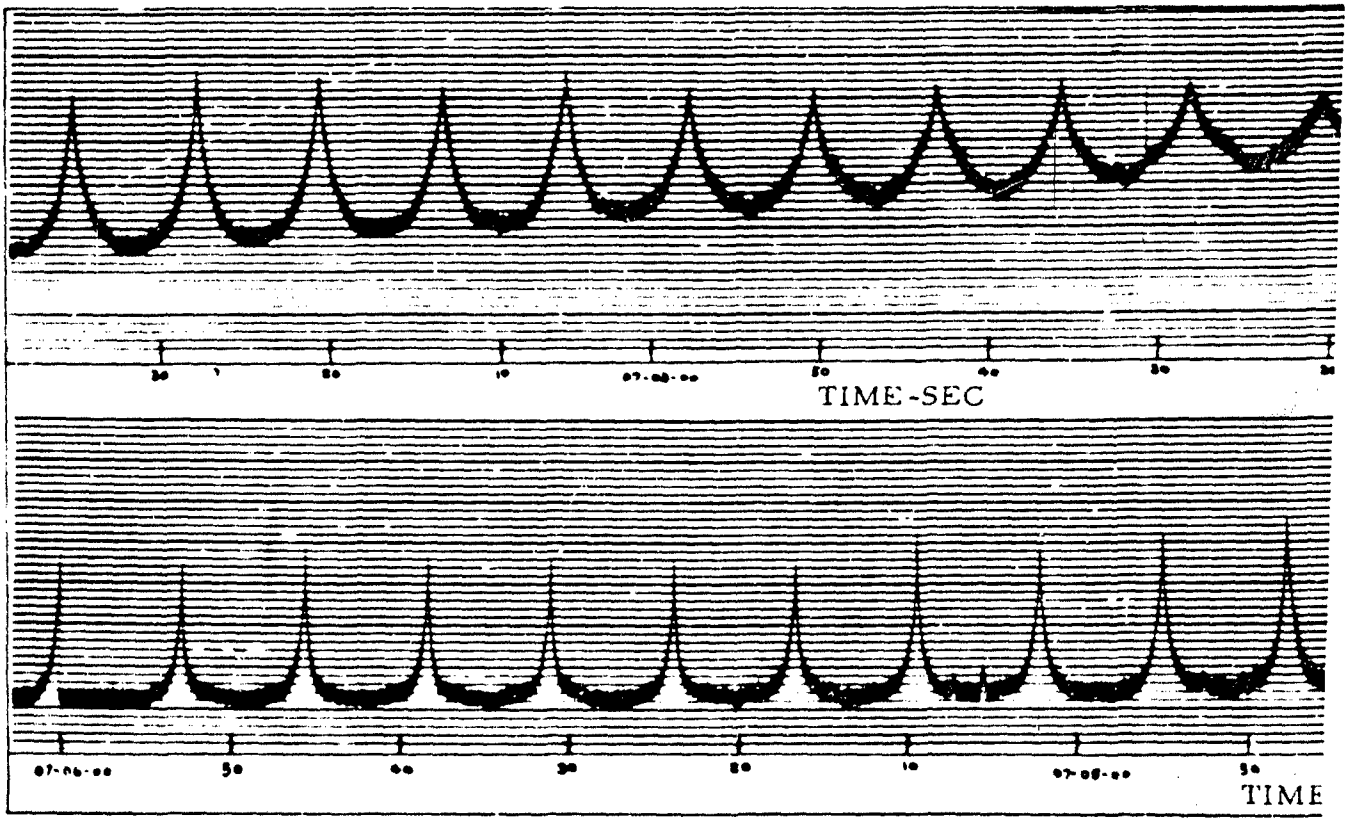

Figure 8

Light curve of 1962 β a2 showing composite diffuse and specular reflection characteristics. Note the repetitive irregularities following $07^h04^m20^s$.

A

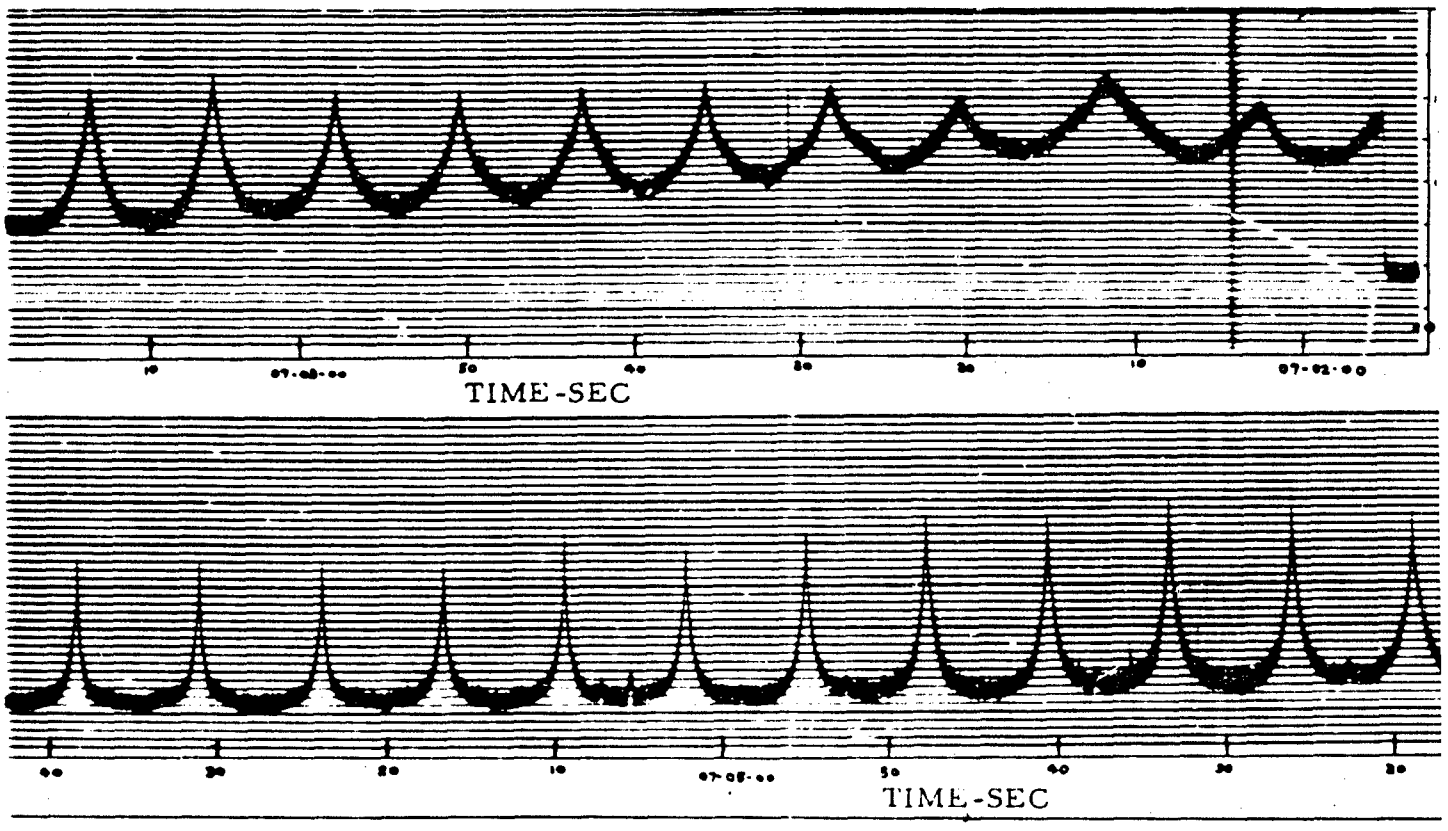

Figure 8

e of 1962 β a2 showing composite diffuse
ar reflection characteristics. Note the
e irregularities following $07^h04^m20^s$.

B

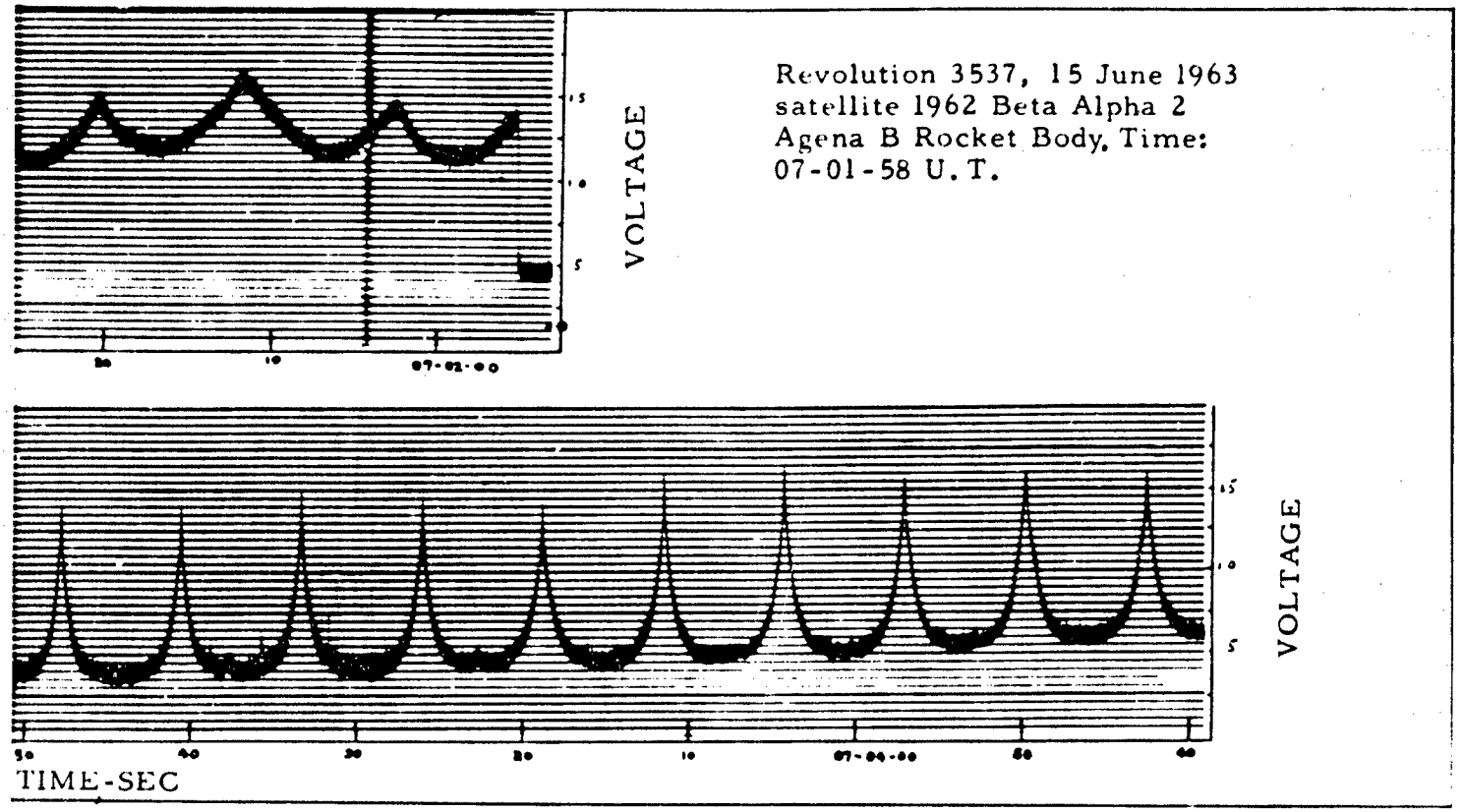
Revolution 3537, 15 June 1963
satellite 1962 Beta Alpha 2
Agena B Rocket Body, Time:
07-01-58 U.T.
VOLTAGE
VOLTAGE
TIME-SEC

C

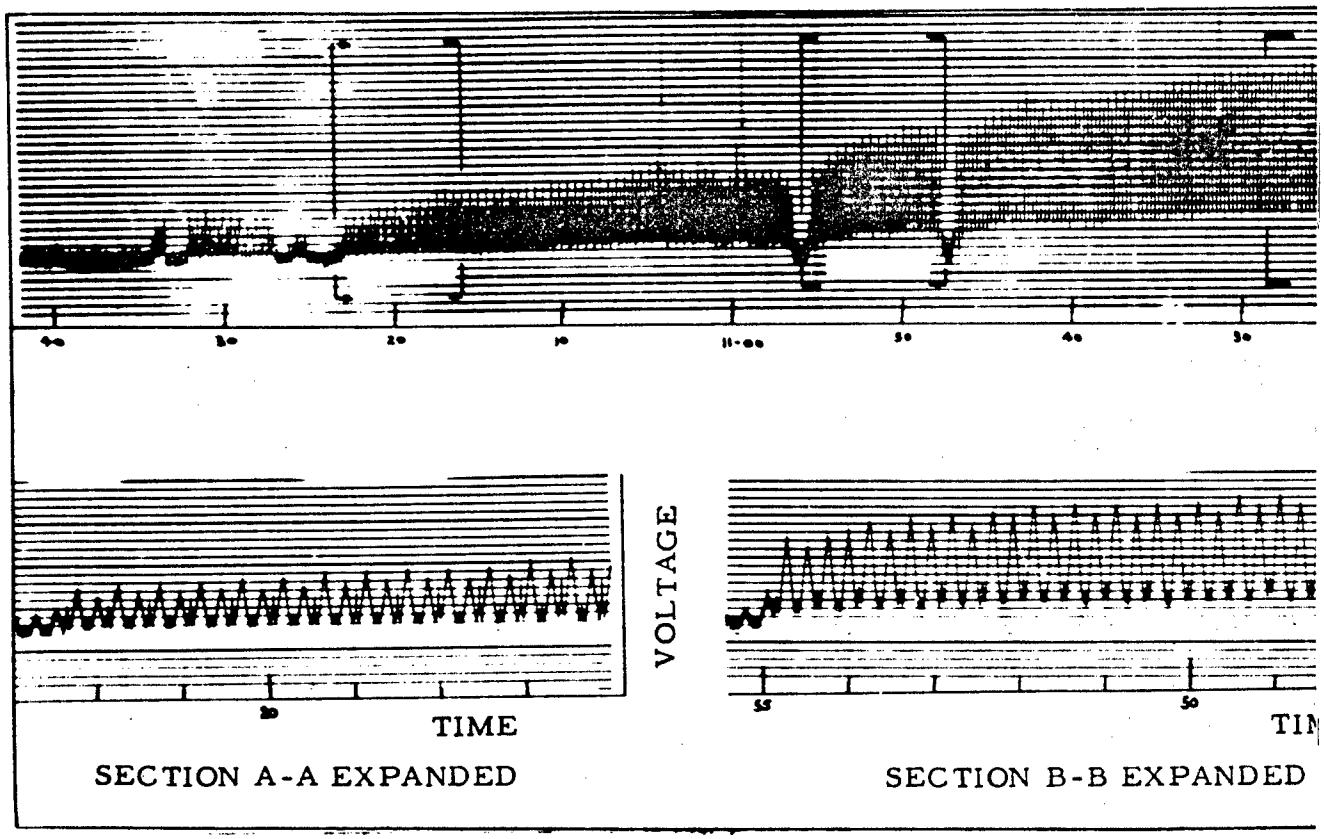

Figure 9

Light curve of 1963-10B showing diffuse reflection characteristic

A

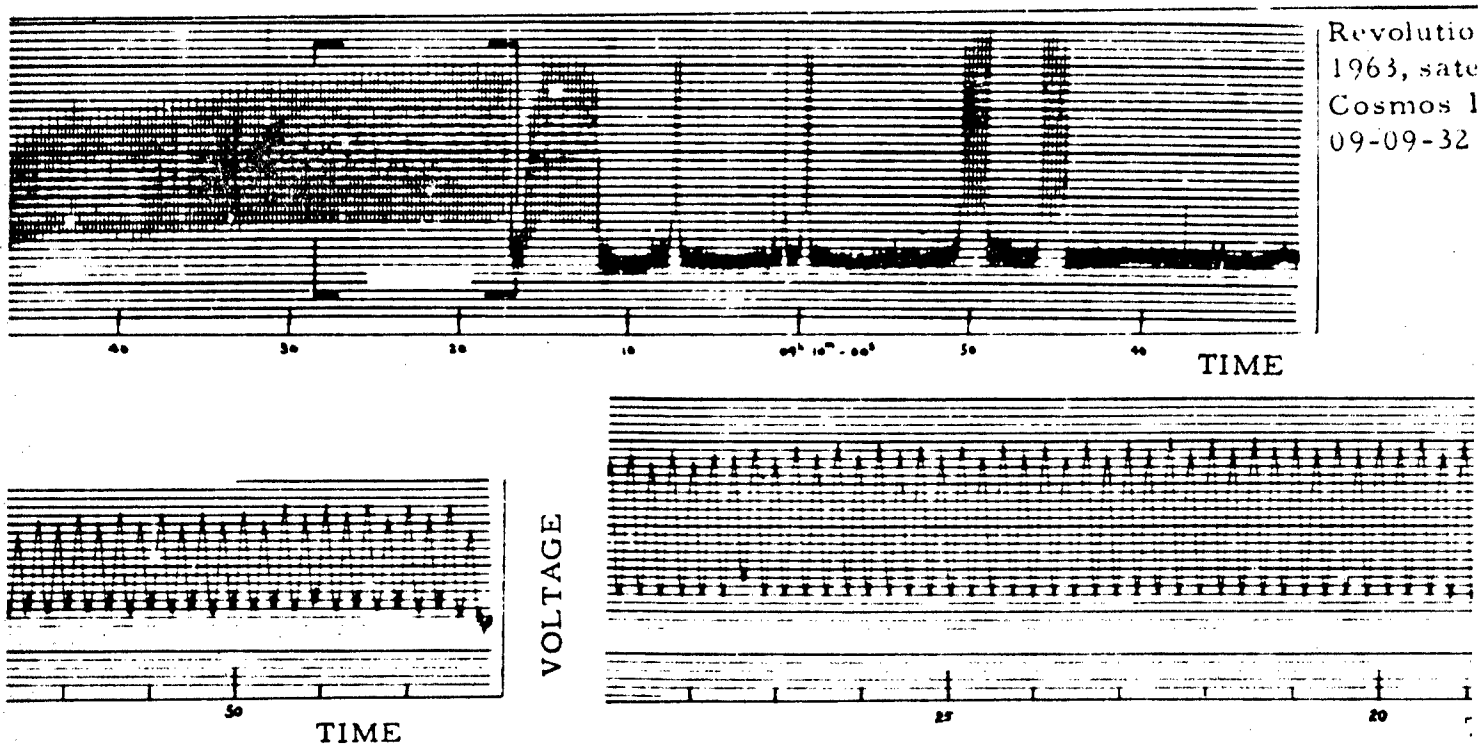

flection characteristic.

B

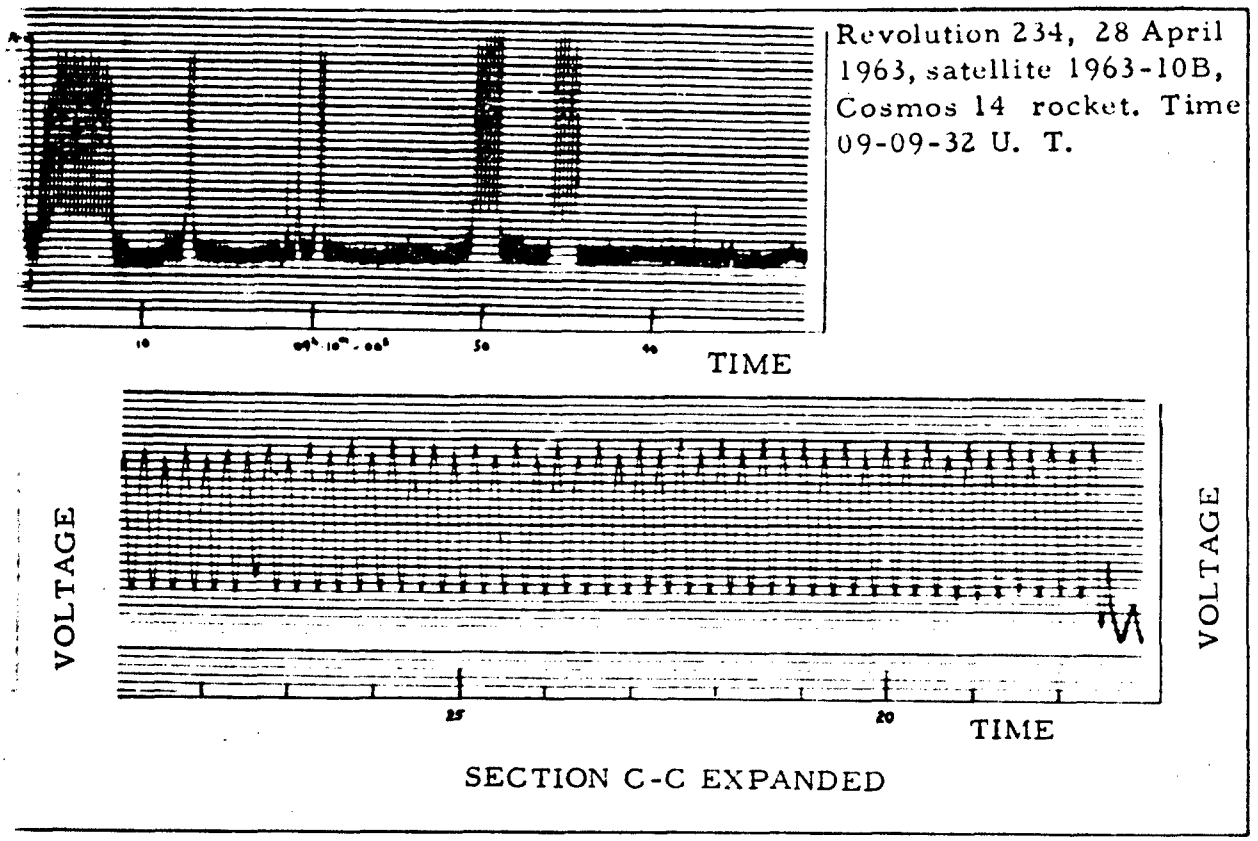
Revolution 234, 28 April 1963, satellite 1963-10B, Cosmos 14 rocket. Time 09-09-32 U. T.
TIME
VOLTAGE
VOLTAGE
TIME
SECTION C-C EXPANDED

C

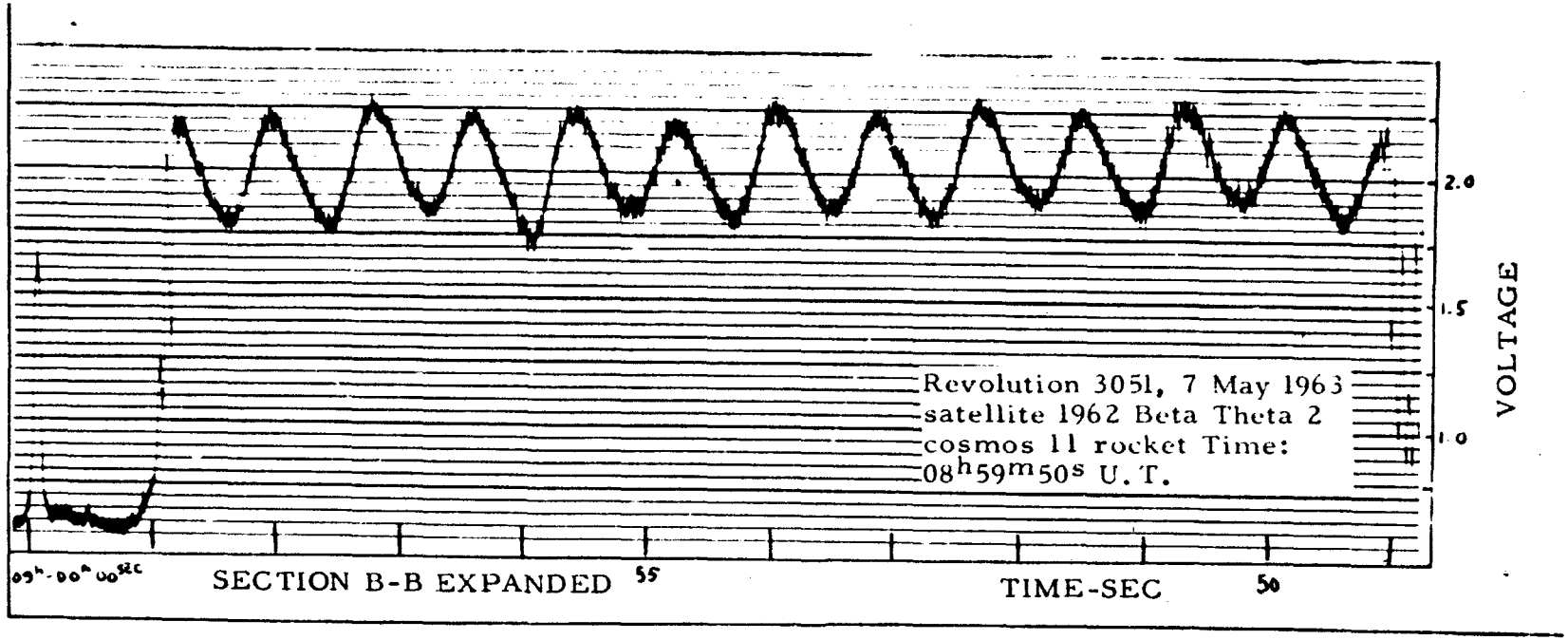

Figure 10

Light curve of 1962 β θ 2 showing diffuse variations of 1.0 mag. superposed on a steady brightness of 2.5 magnitudes.

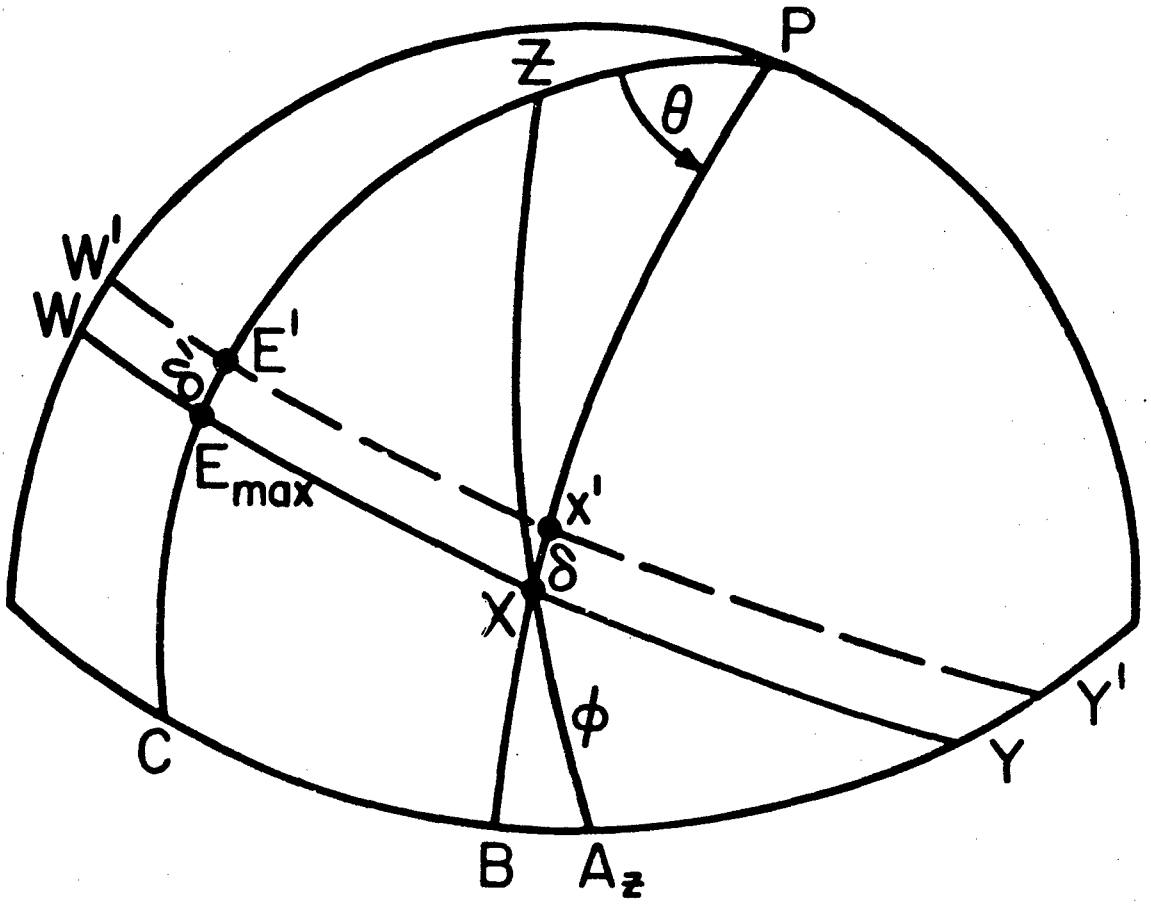

Figure 11

Geometry of Quad-R-Axial mount for satellite tracking.
Satellite traverses path WXY. Mount great circle coincides with W'X'Y'.

great circle lies on the path W' X' Y' which lies a distance δ' above the culmination point of the satellite path E_{max}, i.e.

$E' + \delta' = E_{max}$ — E is measured up from Horizon; δ' is + in same sense as E, i.e. negative in Fig. 11

At all other points along the satellite passage across the sky, the satellite will lie a distance δ below the equator of the tracking system. As the mount rotates about the polar axis, P, the telescope will follow in the vicinity of the satellite's path if the telescope is offset "southward" by the angle δ' so that exact agreement occurs at the polar angle $\theta = 0$. If (1) one varies δ with θ or (2) varies E' with θ during the tracking operation, exact coincidence can be obtained. Clearly both systems must be examined to determine the problems of

(1) Determining E' and δ' for either case
(2) Determining δ (θ) if one tracks with a δ, θ system
(3) Determining E' (θ) if one tracks with an E', θ system

In the above problems one will have knowledge of C, ϕ max, ϕ (Az), Az (t) and no other data. The ϕ and Az data normally will be available from a digital computer as tabular data in the parameter t, (t = time), not as explicit closed expressions. This is in contrast to the Liigant and Einasto technique of generating an approximate orbit from a linearized approximation to the orbital motion, more suitable for analogue control of the telescope.

The problem of the mount motion for the case of the δ, θ system is analogous to the problem of the astronomical triangle, i.e. given the azimuth and elevation, determine the right ascension and declination. The difference lies in the fact that the latitude of the observer and hence the altitude of the pole is unspecified, and must be chosen to fit the apparent path.

Consider the spherical triangle PZX. The following quantities can be established immediately:

$PZ = E_{max} - \delta'$

$PX = 90 - \delta$

$ZX = 90 - \phi$ = Complement of elevation of the satellite

$ZPX = \theta$ = Train Angle = Platform Angle = Track Angle

PZX = Az of satellite from pole of the mount

$= Az - (C + 180) = Az + 180 - C$

By the cosine formula

$\cos ZX = \cos PZ \cos PX + \sin PZ \sin PX \cos ZPX$

$$\cos(90-\phi) = \cos(E_{max} - \delta')\cos(90-\delta) + \sin(E_{max}-\delta')\sin(90-\delta)\cos\theta$$

$$\sin\phi = \cos(E_{max}-\delta')\sin\delta + \sin(E_{max}-\delta')\cos\delta\cos\theta$$

Also by the cosine formula

$$\cos PX = \cos PZ \cos ZX + \sin PZ \sin ZX \cos PZX$$

$$\cos(90-\delta) = \cos(E_{max}-\delta')\cos(90-\phi) + \sin(E_{max}-\delta')\sin(90-\phi)\cos(Az + 180-C)$$

or

$$+\sin\delta = \cos(E_{max}-\delta')\sin\phi - \sin(E_{max}-\delta')\cos\phi\cos(Az-C)$$

So far one has two equations relating θ and δ with ϕ, Az, C, and E_{max} through the parameter δ'.

(1) $$\sin\delta = -\cos(E_{max} + \delta')\sin\phi + \sin(E_{max} + \delta')\cos\phi\cos(Az-C)$$

(2) $$\sin\phi = -\cos(E_{max} + \delta')\sin\delta + \sin(E_{max} + \delta')\cos\delta\cos\theta$$

From the law of sines a third relationship is obtained

$$\frac{\sin PZX}{\sin PX} = \frac{\sin\theta}{\sin ZX} \text{ or } \frac{\sin(180 + Az - C)}{\sin(90-\delta)} = \frac{\sin\theta}{\sin(90-\phi)}$$

$$\sin\theta = \frac{-\cos\phi\sin(Az-C)}{\cos\delta}$$

For each set of coordinates $\phi_i(t)$, $Az_i(t)$ one can establish the simultaneous equations:

(1) $$\sin\theta_i = \frac{-\cos\phi_i\sin(Az_i-C)}{\cos\delta_i}$$

(2) $$\sin\delta_i = \cos(E_{max}-\delta')\sin\phi_i - \sin(E_{max}-\delta')\cos\phi_i\cos(Az-C)$$

(3) $$\sin\phi_i = \cos(E_{max}-\delta')\sin\delta_i + \sin(E_{max}-\delta')\cos\delta_i\cos\theta_i$$

Observe that each new set of apparent topocentric positions ϕ_k, Az_k yields three new equations with only two new unknowns δ_k, θ_k. It is thus possible to determine the parameters E_{max}, δ', and C by selecting at least three sets of apparent topocentric positions. Additional ϕ_i, Az_i sets will allow least-square determination of these three parameters by establishing equations of condition on any or all of the parameters, N topocentric positions will formally yield 3N transcendental simultaneous equations. The solution of these may be most formidable.

The above approach of least square determination of the mount parameters by solution of the simultaneous transcendental equations is essentially equivalent to the variational choice of the approximating small circle orbit

used by Liigant and Einasto. In the present case, one is fitting to the actual apparent trajectory as seen by the topocentric observer, which may be advantageous over the fitting to an intermediate circular approximation, although this is clearly not established. In both approaches the resulting four-parameter coordinate system will yield increasing errors as the orbit becomes more eccentric.

Solution of the simultaneous equations was not attempted. Instead, calculations were made to explore the adequacy of the 4-axis mount by parametric fitting of curves. Both the $E'(\theta)$ and the $\delta(\theta)$ systems were examined with the bulk of the effort directed at the $E'(\theta)$ system, since the existing tracker has a motorized drive on this axis. The method of computation is outlined in Appendix C.

USE OF 4-AXIS MOUNT WITH CROSS TRACK CORRECTION BY E-AXIS VARIATION

Transits of 1962 β a 2 were used to explore the extent to which the quad-r-axial mount would improve the ease of tracking. This vehicle, an Agena B upper stage, is in a near-circular orbit at a height of approximately 1000 km and is an ideal photometric target since it exhibits both specular and diffuse properties. The selected transits were for the Sulphur Grove, Ohio tracking site on revolutions 5465, 5471, 3795, 3808, and 3782 with culmination zenith distance of approximately 0.5, 12.5, 27.8, 46.2 and 68.8 degrees, respectively. These are the same transits whose 3-axis deviations in cross track are shown in Figure 6.

Figure 12 and 13 show the improvements possible for small and large zenith distance. The sensitivity of the improvement on the correct choice of the fourth-axis offset, δ'_o, is quite high. The values used were obtained by iterative solution to pass the small circle through the culmination point and one of the near-horizon points. In general the use of a horizon point near 10-degrees elevation yielded the most linear fit.

Figure 14 is given to allow comparison of the $E'(\theta)$ system with the 3-axis system shown in Figure 6. If the region of stable tracking is defined as deviation of the required crosstrack angle by less than 12 minutes of arc, the quad-r-axial $E'(\theta)$ system provides an increased duration of stable tracking by a factor of at least four, in the examples chosen from less than 2 minutes of time to in excess of 8 minutes of time (approximately 4.5 minutes each side of culmination regardless of the culmination zenith distance). Outside these limits the additional setting axis continues to reduce the corrections appreciably.

USE OF 4-AXIS MOUNT WITH CROSSTRACK CORRECTION BY δ-AXIS VARIATION

Although a quad-r-axial mount using correction at the elevation axis ($E'(\theta)$ variation) shows marked improvement over the 3-axis mounting, an abrupt break still occurs at large track angles. This is due to the same fault which is inherent in the 3-axis mount, namely that the pole of telescope rotation is moved with the adjustment $E(\theta)$ and hence the satellite's motion is increasingly in a plane not normal to the axis of tracking rotation. If the fourth axis, δ, is continuously adjusted while maintaining a fixed pole of telescope rotation, this effect should be reduced.

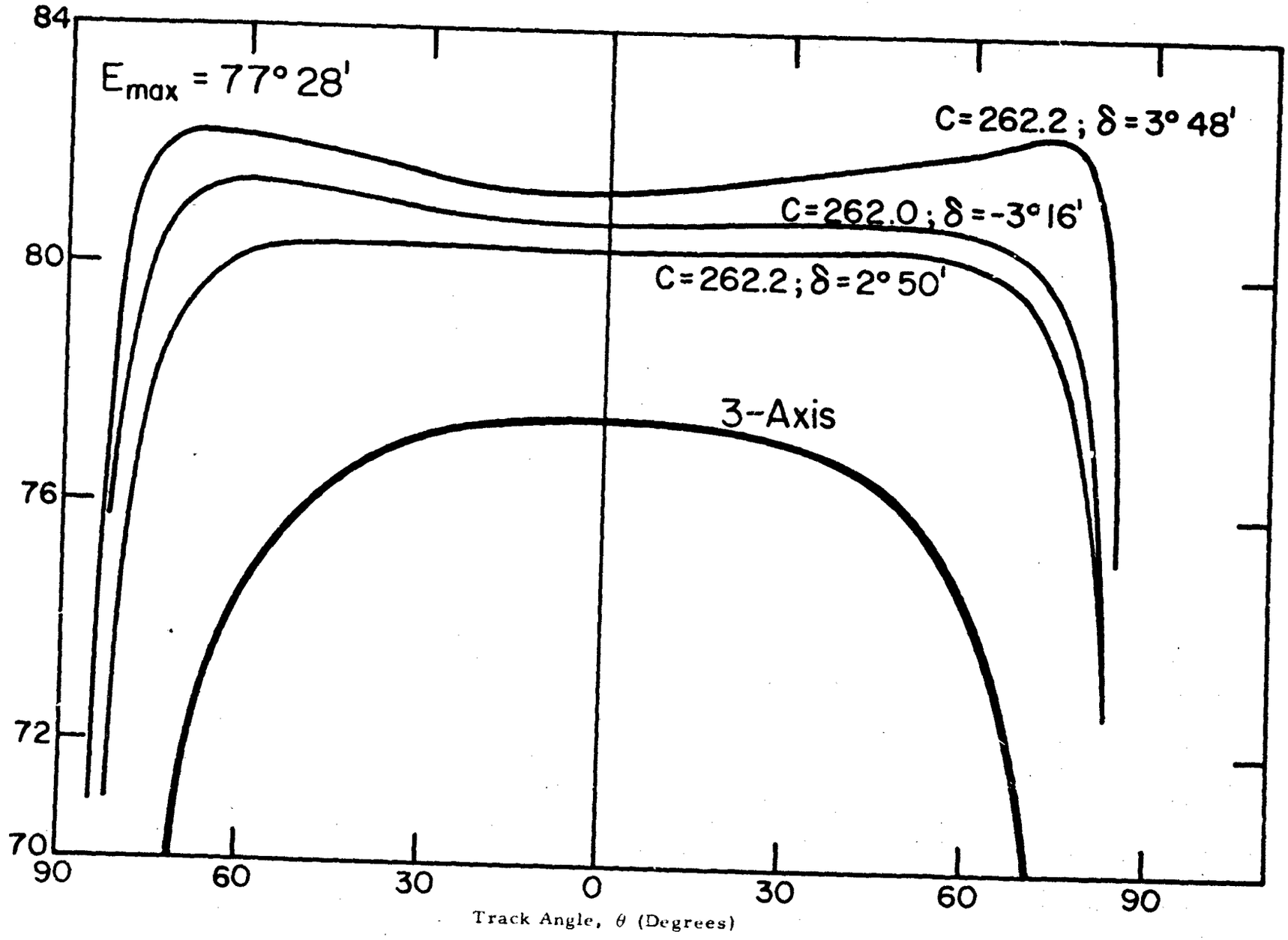

Figure 12

Reduction of crosstrack rotation with E'(θ) quad-r-axial system for small zenith-distance transit. E[illegible] = 77° 28'

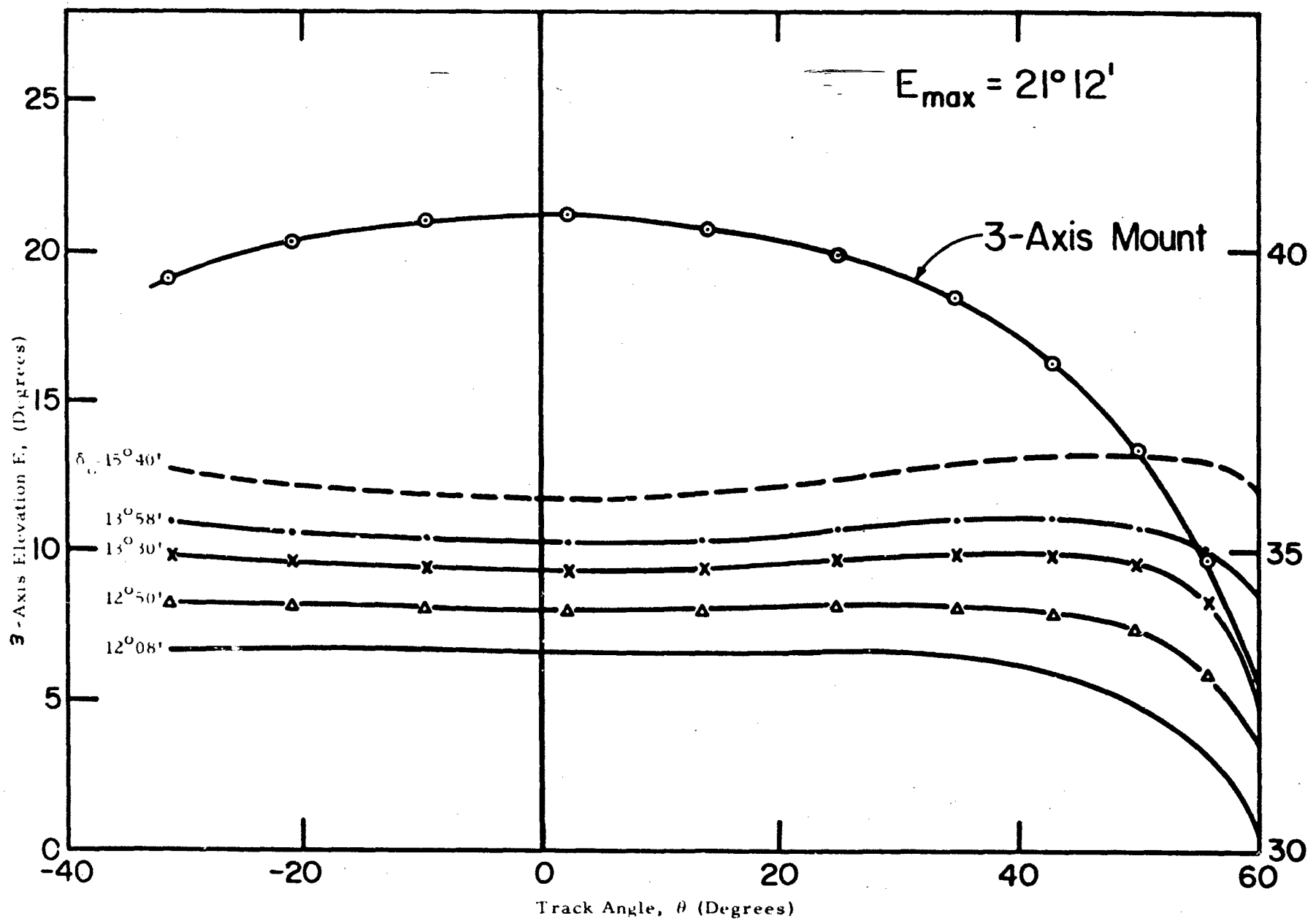

Figure 13

Reduction of crosstrack rotation with E' (θ) quad-r-axial system for large zenith-distance transit, E_{max} = 21° 12'.

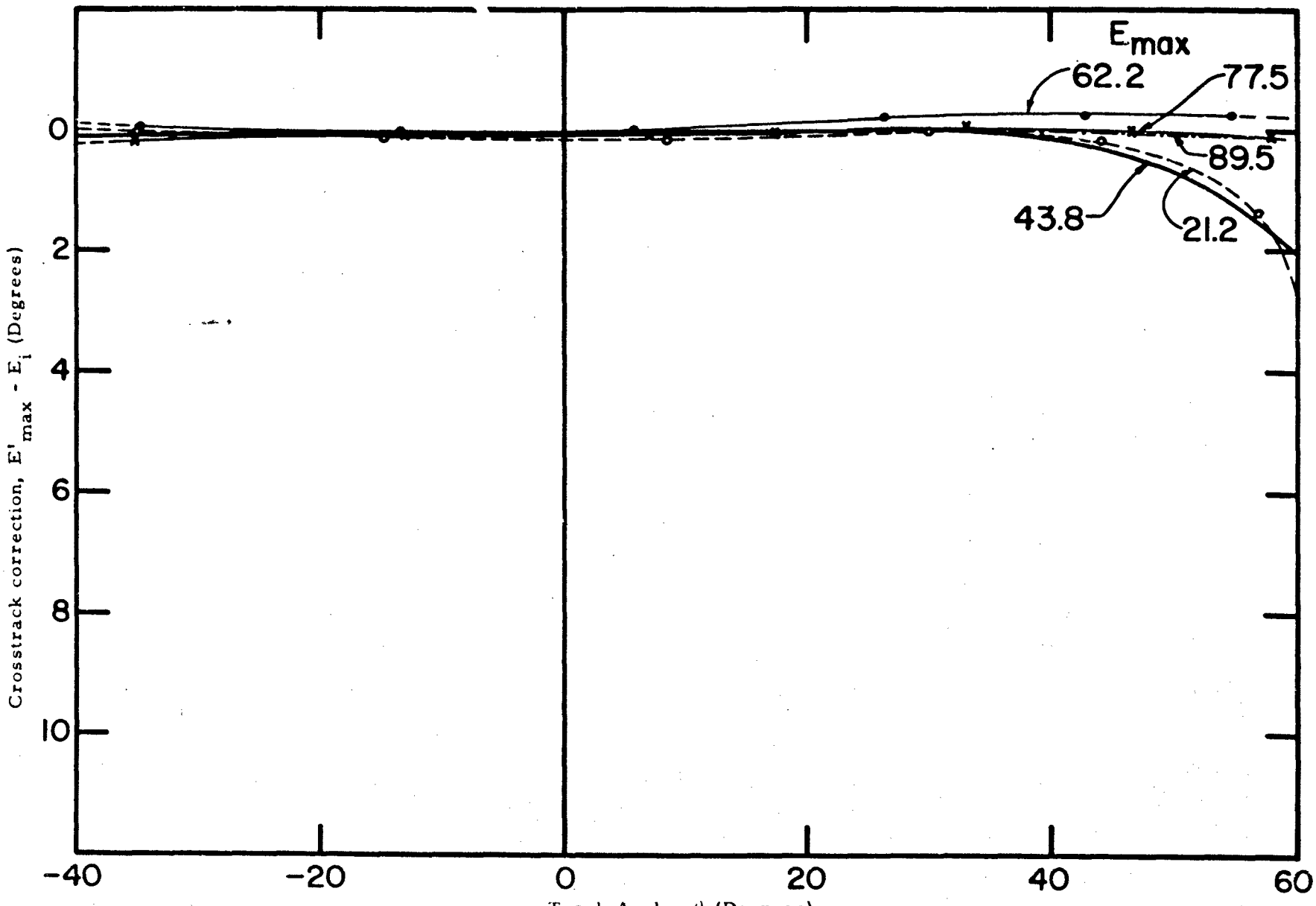

Figure 14

4-Axis crosstrack corrections with E'(θ) system as a function of track angle and elevation

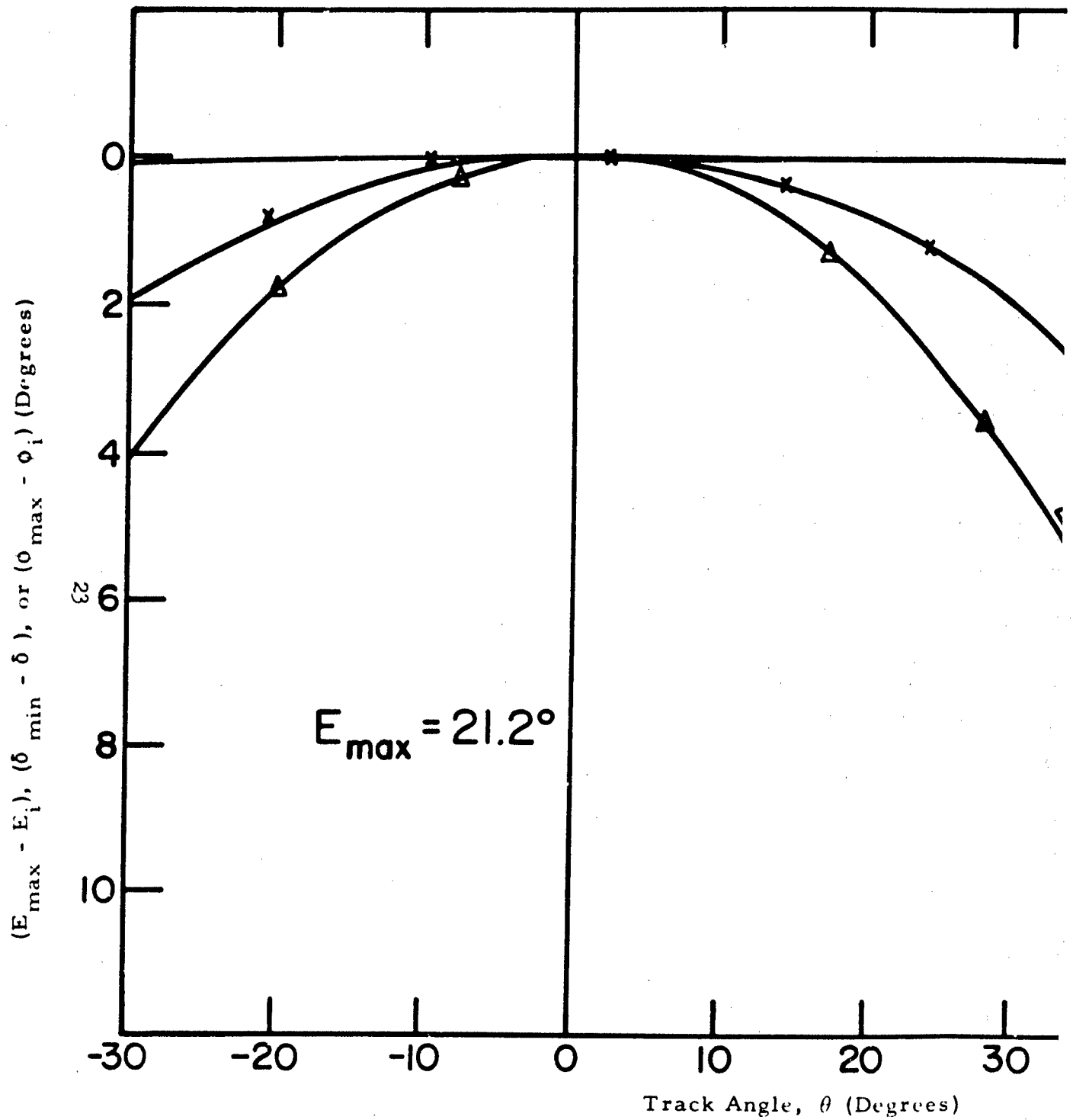

Figure 15

Comparison of crosstrack corrections for 2, 3, and 4-axis tracking transit of 1000-kilometer, near-circular satel

A

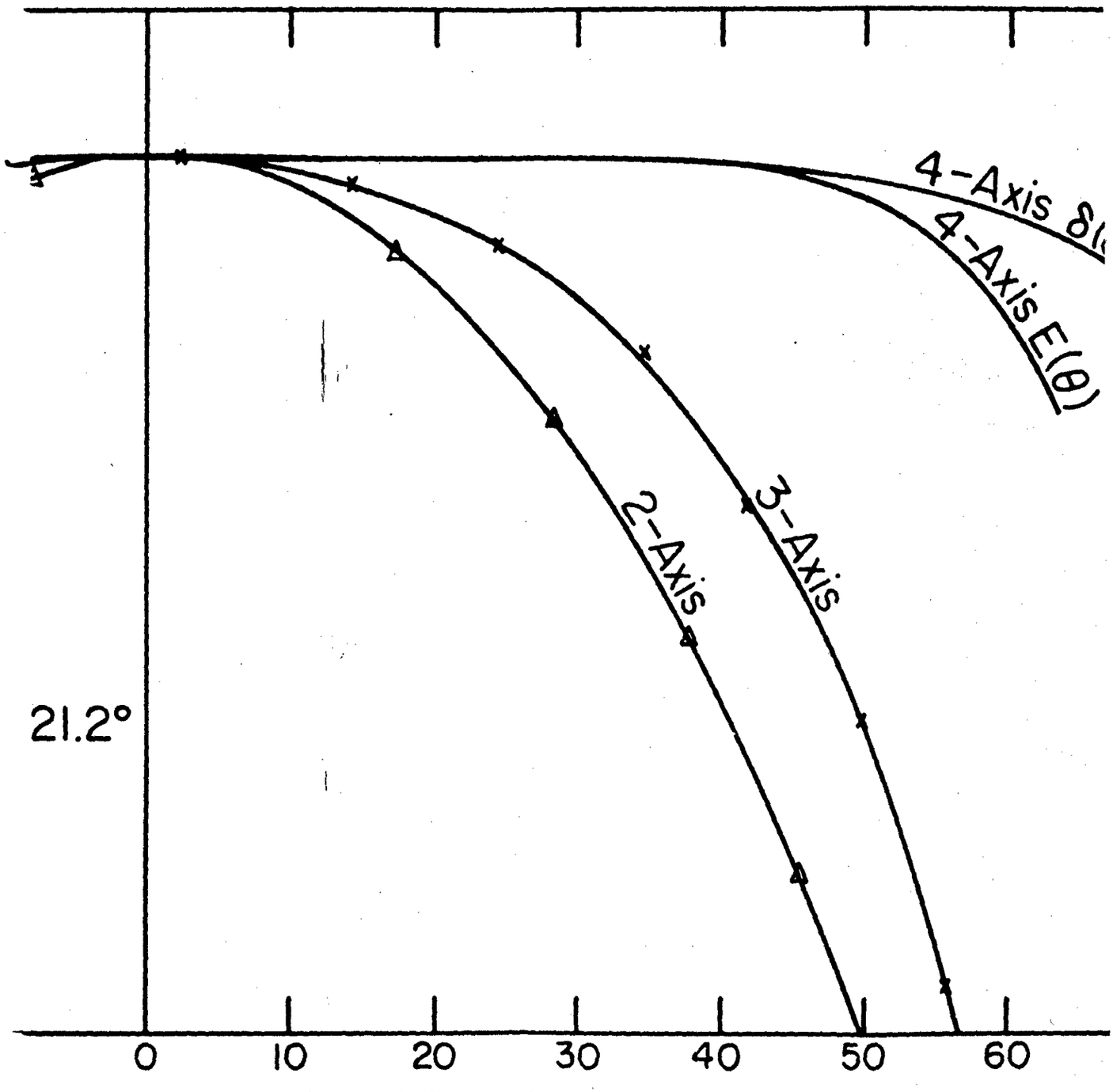

Figure 15

osstrack corrections for 2, 3, and 4-axis tracking mounts for low-elevation transit of 1000-kilometer, near-circular satellite.

B

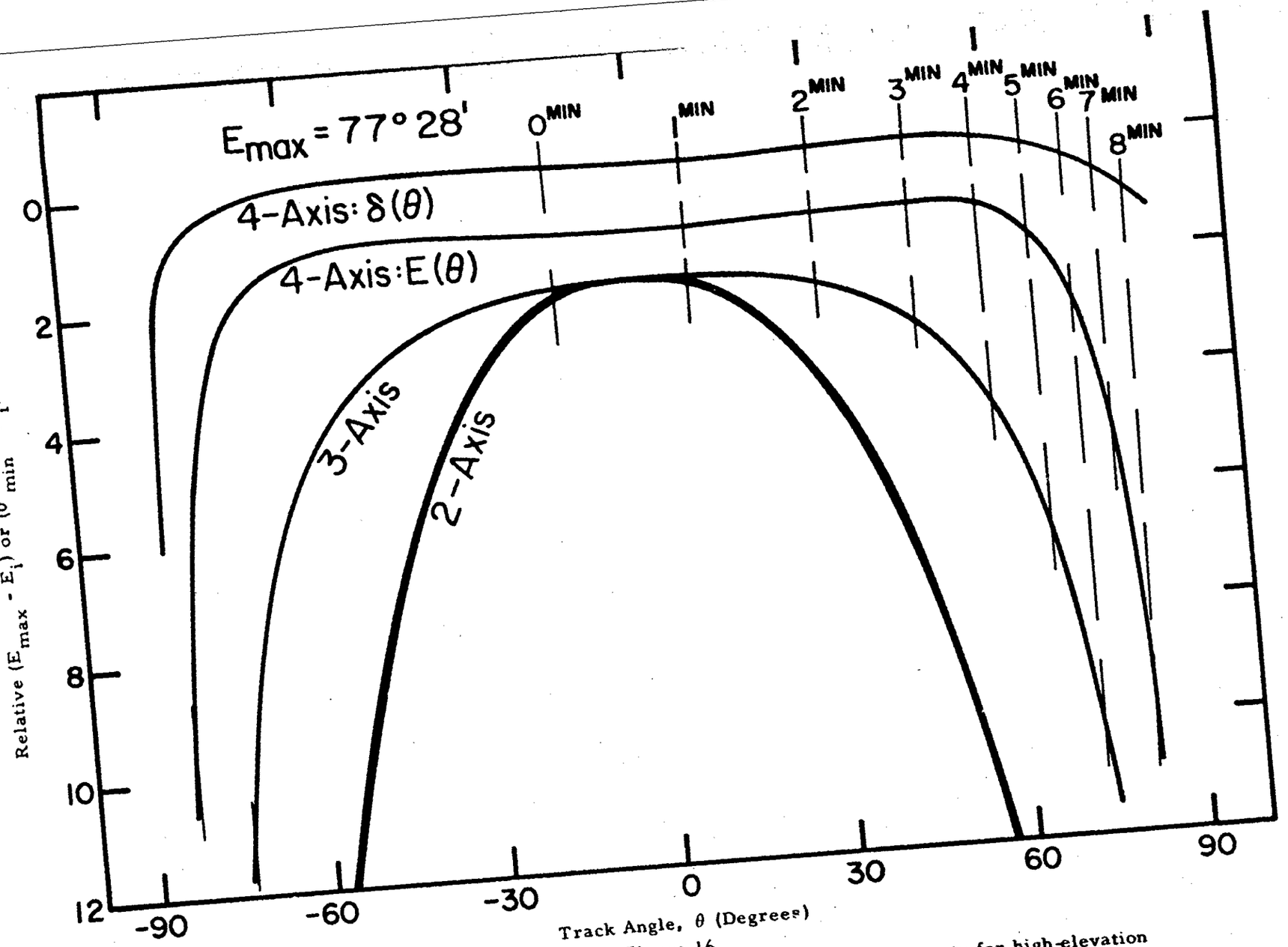

Figure 16

Comparison of crosstrack corrections for 3 and 4-axis tracking mounts for high-elevation transit of 1000-kilometer, near circular satellite.

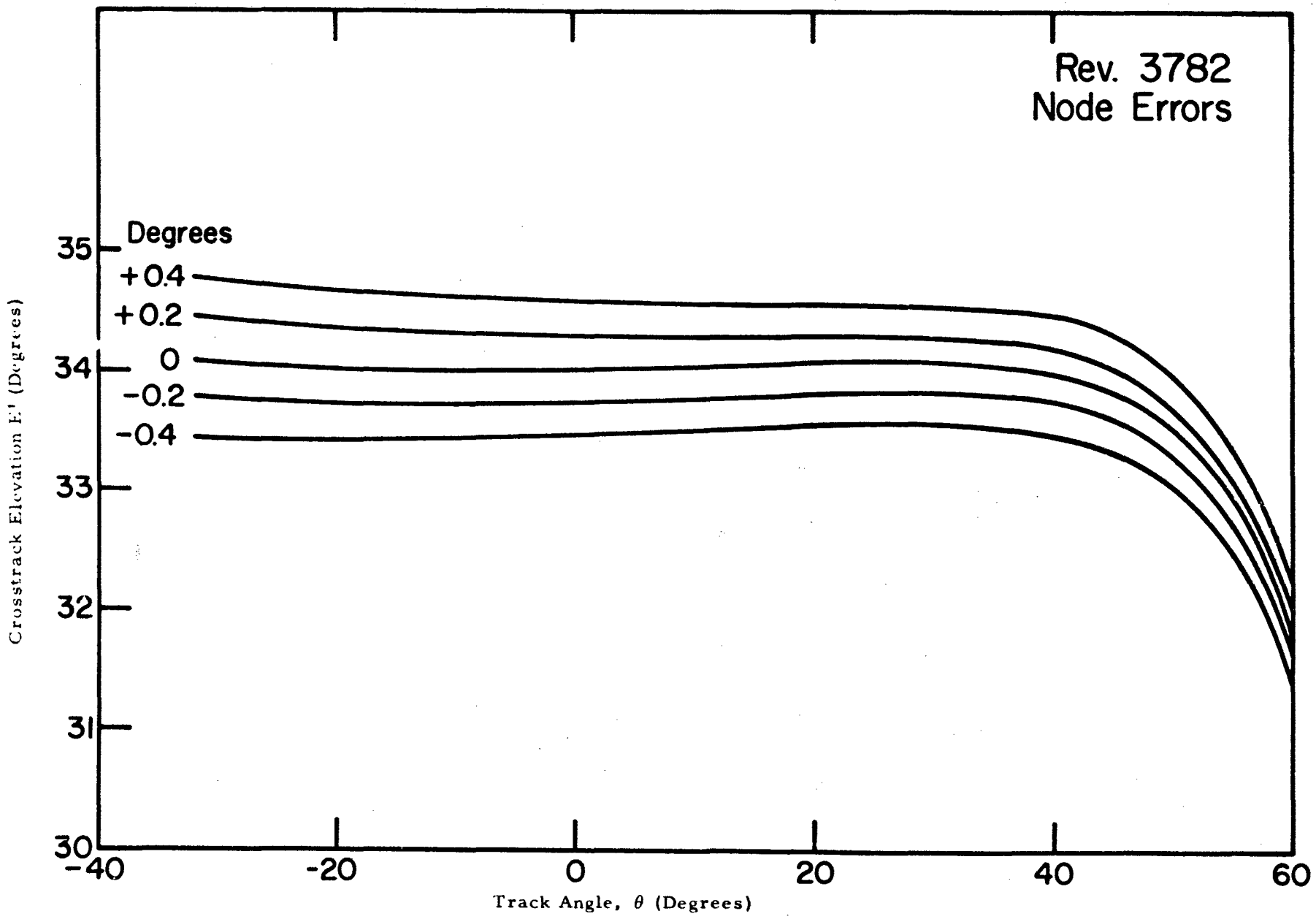

Figure 17

Effect of error in location of the orbital node on the required crosstrack setting of E'(θ) system. Maximum elevation of nominal transit 21° 12'.

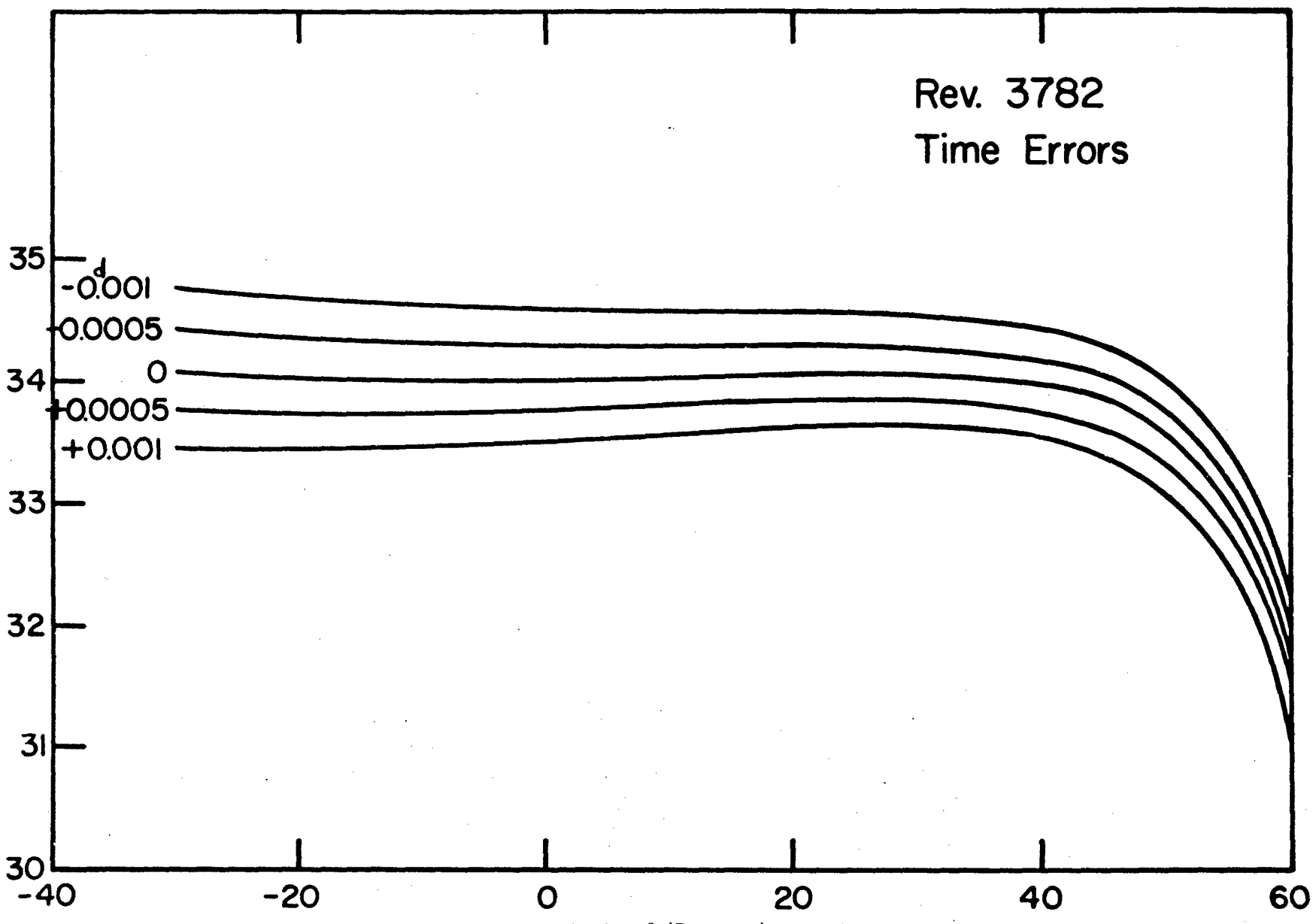

Figure 18
Effect of error in time of nodal crossing on the required crosstrack setting of E' (θ)

Figure 15 and 16 show this to be the case. There is no appreciable improvement in tracking near culmination, when the two adjustment axes are essentially coincident, but at extreme track angles the $\delta(\theta)$ system is distinctly superior for transits at both large and small culmination zenith distances. The curves of Figure 16 are separated to emphasize the relative duration of stable tracking.

SENSITIVITY OF 4-AXIS TRACKING TO PREDICTION ERRORS

Before electing to adopt a 4-axis mount, it is of importance to consider the effects of the prediction errors which will always exist to some degree. To investigate whether moderately large errors in the orbit elements would negate the gains to be expected from the additional degree of freedom, a set of perturbed look-angle computations were obtained for Rev. 3782 of 1962 β α 2, the lowest culmination transit of Fig. 6, i.e. the transit gaining most linearization from the additional setting axis. Two elements were perturbed by realistic values; the location of the ascending node was displaced by values of $\pm$ 0.2 and 0.4 degrees in right ascension and the time of nodal crossing by $\pm$ 0.72 and 1.44 minutes. Based on personal tracking experience, most space vehicles are under better control than this when not yet near final atmospheric decay. Figure 17 and 18 show the effects of these perturbations on the cross-track axis settings when the offset angle δ is fixed at the value chosen for the nominal elements. The effects of early or late arrival or error in location of the orbit plane are observed to be nearly equivalent (as would be expected by rigidity of trajectory arguments) and are observed to be primarily a simple shift of the mean crosstrack angle to be used during the transit. A slight cross-track velocity is introduced, but it remains on the order of the corrections already necessary for the nominal orbit. A field aperture of 5-6 minutes of arc would allow five minutes of photometry without crosstrack correction in any of the cases chosen. The 4-axis mount remains a valuable asset even for vehicles with relatively large predictions errors. While the results shown are for the $E(\theta)$ system, the conclusion is equally valid for the $\delta(\theta)$ system.

CONCLUSIONS

From the foregoing it is apparent that a quad-r-axial mounting is much to be preferred over a 3-axis system for the purpose of satellite photometry whether guiding is by manual or by automatic or semi-automatic control. The photometry of faint targets will require the use of apertures closer to one square minute of arc in area. This would place the sky background at + 10 stellar magnitudes. With skill the observer can track within these limits, particularly if a slotted aperture is used instead of circular one in order to gain tolerance in the track angle direction.

It is planned to modify the present Nunn mounting by the addition of an inner gimble, and to install a 24-inch optical system with a δ-axis drive to obtain full benefit of the quad-r-axial mount.

ACKNOWLEDGEMENTS

The author wishes to acknowiedge the valuable assistance of Mrs. Rhonda Duvall in performing many of the computations in this analysis. Grateful acknowledgement is also made to the C.M. Sgt E.T. Tyson of the Avionics Laboratory, USAF for the design, establishment, and later transfer to the author of the entire photometer system at the ARL Field Site after completion of his experiments. Thanks also go to Mr. C. Rosenberger and T. Sgt. A.

Jarvis for assistance in collecting photometric data, to Capt. E. M. Vallerie III for use of the photometric data used in this paper, and to Mr. Robert Chabot of the SPACETRACK R & D Center, USAF for the special calculations with perturbed orbital elements.

BIBLIOGRAPHY

1. V. P. Tsesevich, "On Brightness Variations of Artificial Satellites", Trans. of IAU, X, (1958), p. 722.

2. V. M. Grigorevskij and U. Gyunttsell Lingner, "Optical Observation of Artificial Earth Satellites," NASA Technical Translation F-11, February 1961, pp. 1-18.

3. M. Melin, "The Tumbling of 1958 δ 1," Sky & Telescope XVIII, No. 2, (Dec 1958), pp. 82-3.

4. M. Melin, "More About Project Rotor", Sky & Telescope XVIII, No. 3, (Jan 1959), pp. 145-6.

5. J. G. Moore, "Photometric Observations of Satellite 1958δ1", Sky & Telescope XVIII, No. 2, p. 83.

6. S. V. Venkateswaren, J. G. Moore, and A. J. Krueger, "Determination of the Vertical Distribution of Ozone by Satellite Photometry," J. Geo. Res., 66, (June 1961), pp. 1751-71.

7. "Telstar Spin Axis Studies", Sky & Telescope XXV, No. 3 (March 1963), p. 143.

8. J. S. Courtney-Pratt, D. W. Hill, J. W. McLaughlin, and J. H. Hett, "Optical Measurements on Telstar", A. J., 68, No. 2, (March 1963), p. 70.

9. W. C. Jakes, Jr., "Participation of the Holmdale Station in the Telstar Project," NASA SPL 32, Vol. 2 (June 1963).

10. R. J. Davis, R. C. Wells, F. L. Whipple, "On Determining the Orientation of a Cylindrical Artificial Earth Satellite," Astronomica Acta, 3, (1957), p. 231.

11. R. H. Giese, "Altitude Determination from Specular and Diffuse Reflection by Artificial Satellites. SAO Research in Space Science Special Report No. 127, (July 1963).

12. R. H. Wilson, Jr., "Optical & Electronic Tracking" Geophysical Monograph No. 4, A.G.U. (1959), pp. 67-78.

13. E. M. Vallerie III, "Investigation of Photometric Data Received from an Artificial Earth Satellite". Thesis, AFIT, August 1963.

14. K. G. Henize, "Tracking Artificial Satellites and Space Vehicles", Advances in Space Science, Vol 2, F.I. Ordway III, Editor, Academic Press, New York (1960).

15. M. Liigant and Ya. Einasto, "Theory of Automatic Satellite Tracking Telescopes", Soviet Astronomy-A. J., 4, No. 6, (May-June 1961) pp. 1023-1031.

APPENDIX A

INTRODUCTION

Although over six and one-half years have elapsed since the first orbiting of near-earth satellites, observation of satellites by optical means is still restricted to techniques allied closely to astrometry, i.e., the location and cataloging of satellites by the position in space with only minor concern for the apparent brightness and color of the satellite. Faint satellites and slowly tumbling satellites, varying widely in brightness, cause special difficulties in visual or photographic astrometric observation but no serious attempt has been made in the recording of light curves of orbiting vehicles other than for a few exploratory, and generally very specific, purposes. The most important of these are outlined below.

1. A brief report in the 1958 I.A.U. Proceedings[1] and a series of four papers[2] appeared in Astronomic Council of the Academy of Sciences of the USSR Bulletin of Stations for Optical Observation of Artificial Earth Satellites, Moscow, No. 10 (1959) discussing the use of photometric data in determination of the orientation in space of Sputniks II and III during 1958. The data used were obtained by visual estimates of skilled observers. Visual observation allowed collection of only a relatively small number of data points but, by use of data from 3-4 observers, mean values of reasonable reliability were obtained. The results given in these papers pointed the way toward some of the data handling necessary for utilization of passive optical data for determination of spin-axis and vehicle-axis orientation.

2. An effort[3,4] for U.S. observers was undertaken in 1958 by the Research Station for Satellite Observation at Harvard College Observatory under the name Project Rotor. Observations were sought of the times of apparent maximum brightness of the Sputnik III rocket carrier as measured at various geographic locations for correlation to obtain equal angles of the longitude axis to the observer/ sun directions as seen from the satellite, using the model of a long, polished cylinder for the rocket. No results were published to the author's knowledge.

3. J. G. Moore, Atmospheric Physics Branch, NOTS, China Lake, California obtained photoelectric light curves[5] of Sputnik III rocket body, using a photometer originally designed for airglow research. Tracking was manual using an auxiliary Askania theodolite mounting. The field aperture was approximately 0.25 degrees. Five transits were recorded during a three-month interval and the results used to measure the damping of the satellite's rotation about its center of mass.

This same type of photometer was later used[6] to measure differential atmospheric extinction of light at selected wavelengths where one pass band coincided with an ozone band. The differential extinction was analyzed to determine the distribution of ozone with height as the satellite reflected light through

successively longer paths of the atmosphere at greater and greater zenith distances. Satellite 1960 ι 1 was used as the target.

4. J. S. Courtney-Pratt[7,8,9] at Bell Telephone Laboratories installed clusters of plane and fluted mirrors on the Telstar satellite to reflect sunlight to a ground telescope equipped with a photoelectric photometer. By selection of variable spacings of the mirrors, the resulting flashes are time-sequence-coded such that the orientation of the spin axis could be deduced to within one degree. Spin rates of 3 revolutions per second resulted in flashes of only some 500 microseconds duration, with brightness ranging from 6.5 to 11th magnitude depending upon range, extinction, and other factors. The detecting telescope was a 12-inch Cassegrain instrument on an alt-azimuth mounting, servo-coupled to an 18-foot tracking antenna and a smaller optical guiding telescope. The tracking accuracy thus achieved would permit use of a 0.5-degree field aperture to limit sky-background signals. Only brief abstracts of this work have been published up to this time.

5. During mid-1962, E. T. Tyson and others of the USAF Avionics Laboratory constructed a two-channel photoelectric photometer for the initial purpose of (1) verifying an increased frequency in stellar scintillation if one observes a spherical, specular satellite and (2) establishing the level of scintillation of large-area diffuse satellites. ECHO I and Explorer IX, the 12-foot aluminized balloon, and several USSR and US upper stage rockets and payloads were photometered, some with ease and others with difficulty. The apparatus is described more fully below but briefly consisted of two 12-inch Cassegrain optical systems mounted on a modified Baker-Nunn satellite camera triaxial mount. Acquisition and tracking were effected by an auxiliary finder telescope with a 2.2-degree field of view. Acceptance of the satellite by the photometer aperture was indicated by modulation of an audio tone by the increase in illumination of the photocell. Tracking was effected with apertures of 2 minutes of arc on vehicles at 1500 km slant ranges and 15 minutes of arc at 300 km slant ranges. Most of this work remains unpublished.

Work with this same apparatus is being continued by the author and others to collect data for use in (1) comparing gross signatures of similar vehicles, (2) attempting spin axis and vehicle orientation solutions by extension of the work of Grigorevskij, and (3) study of methods to improve the quality and quantity of data by improvements in technique.

Other proposals for use of optical photometry have been made from time to time. Indeed the earliest suggested use of the photometric properties of a specular, cylindrical artificial satellite was advanced by Davis, Wells, and Whipple[10] before the orbiting of the first Sputnik. R. H. Giese[11] expanded on the treatment of such vehicles by use of bursts of specular flashes as noted by visual observers or from camera films. Giese also explored parameters affecting the light curves of diffusely scattering cylinders. One of R. H. Wilson's proposals[12] is embodied in the Telstar experiment, i.e. the use of flat mirrored surfaces to increase the satellite brightness and the timing of flashes to determine orientation.

In general, the application of photometric data is limited by the form, quality and quantity of data available. As is well known in variable star photometery,

visual estimates require the careful use of nearby photometric standard stars which are chosen to eliminate the personal equation of the observers. The accurate timing of brightness peaks by visual observers is unreliable for similar reasons owing to anticipation and reflex errors in the observer. The light curves of space vehicles can be usefully interpreted only if relatively com plete data can be collected by photoelectric methods. As the experience cited above has shown, the photoelectric photometry of space vehicles requires mor precise tracking of the vehicle than that required for astrometric applications. This is necessitated by the small field apertures which must be used to reduce the sky background to levels which are at least as low as the satellite signal at its minimum brightness. The small apertures will also reduce the occurrence of false signals due to near occultations of bright stars.

One other effect has been noted in the course of the photoelectric observati outlined above. This is the inability of the eye to detect brightness fluctations a satellite which do not exceed one stellar magnitude or possibly more. As an example of this, at the instant of recording of the data in Figure 10, the author judged the vehicle as steady in brightness through a 9-inch reflector. Prior to this observation the author had at times been surprised at the apparent constan of brightness over large portions of a certain transits of many of the cylindrica vehicles such as the Sputnik III rocket carrier. This makes impossible the use of visual observations to estimate the instants at which the vehicle spin axis is the coplanar bisector of the observer, satellite and sun angle. The detection o such an invariant brightness during the transit of a diffuse or specular cylindri vehicle would yield a unique determination for the spin axis. Even a nearly in- variant condition would allow a reasonable determination of the spin axis.

APPENDIX B

As mentioned previously the photometer system now in use at the ARL Fie Site is attached to a modified Nunn mount. The 12-inch optical system has 50- percent center blocking, yielding an effective aperture of approximately 10 inc Apertures of 1, 2, 4, 8, and 16 minutes of arc are available in the simple phot meter head to restrict the field of view and consequently the total sky backgrou radiation seen by the photomultiplier. A selected RCA 7029 phototube is used. This design uses an S-17 photocathode which peaks at 5000 Å and is especially suited for use under high ambient light levels. The photomultiplier is energize by a Sweet-type logarithmic feedback power supply which maintains a constant output current from the photocell by regulating the dynode voltage. This gives roughly linear response in stellar magnitudes over a range of 10-15 magnitudes and effectively prevents overloading of the photomultiplier by accidental over exposure. The dynamic response of the photometer electronics is flat to approximately 5000 cycles.

The feedback voltage of the photometer circuit, which is the nearly linear signal output, is fed to an FM tape recorder with a 37 KC center carrier. The two-track Ampex recorder places the lower sideband on one track and signals from a local crystal clock or WWV on the other. The clock is rated with WWV and pulses derived from the clock made coincident with WWV through a delay generator such that local WWV time is impressed directly on the tape with an error of a few hundred microseconds. The tape output is displayed on a Honey- well Visicorder with 1 KC galvanometers. It is expected that the output display

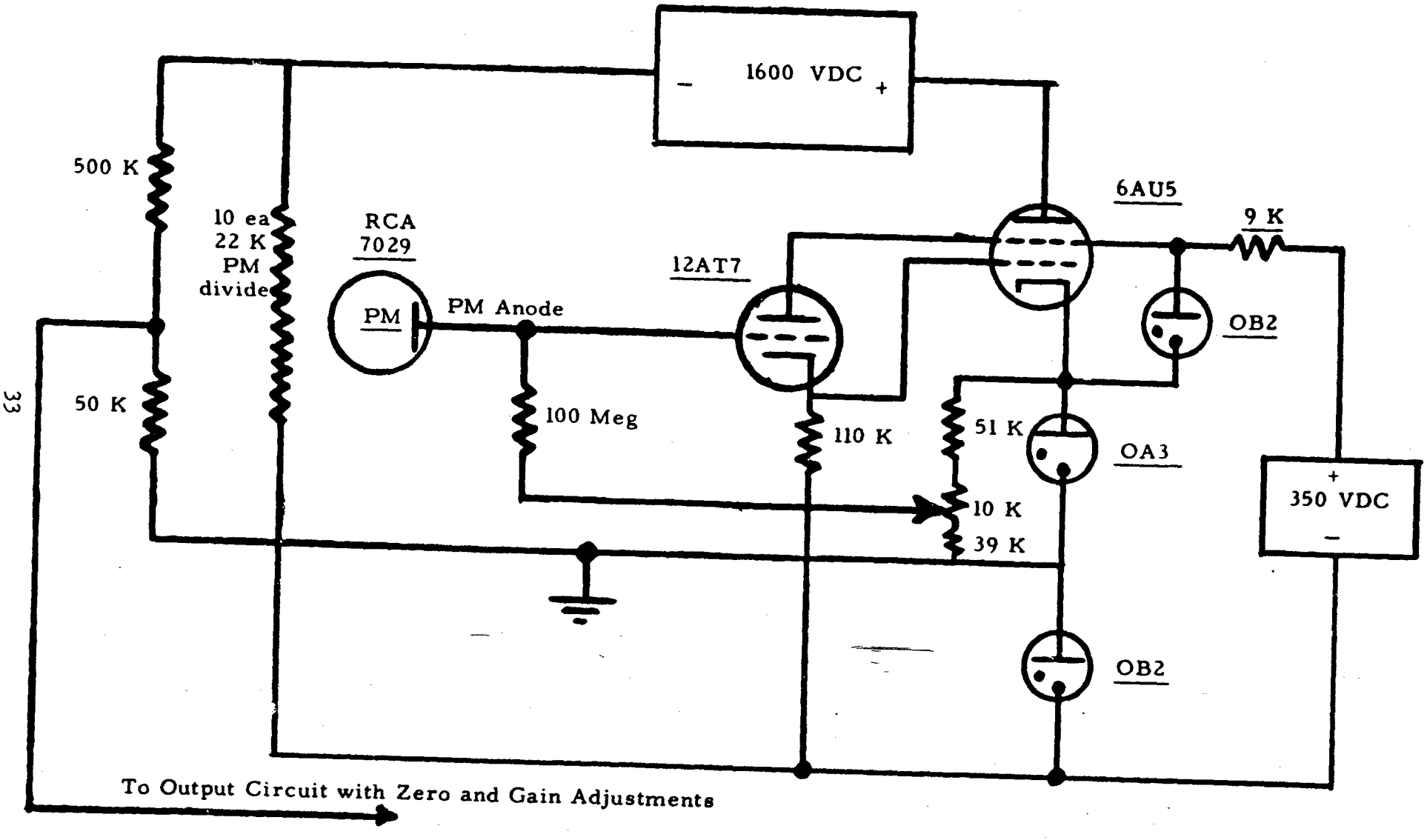

Figure 19. High-frequency logarithmic photometer circuit.

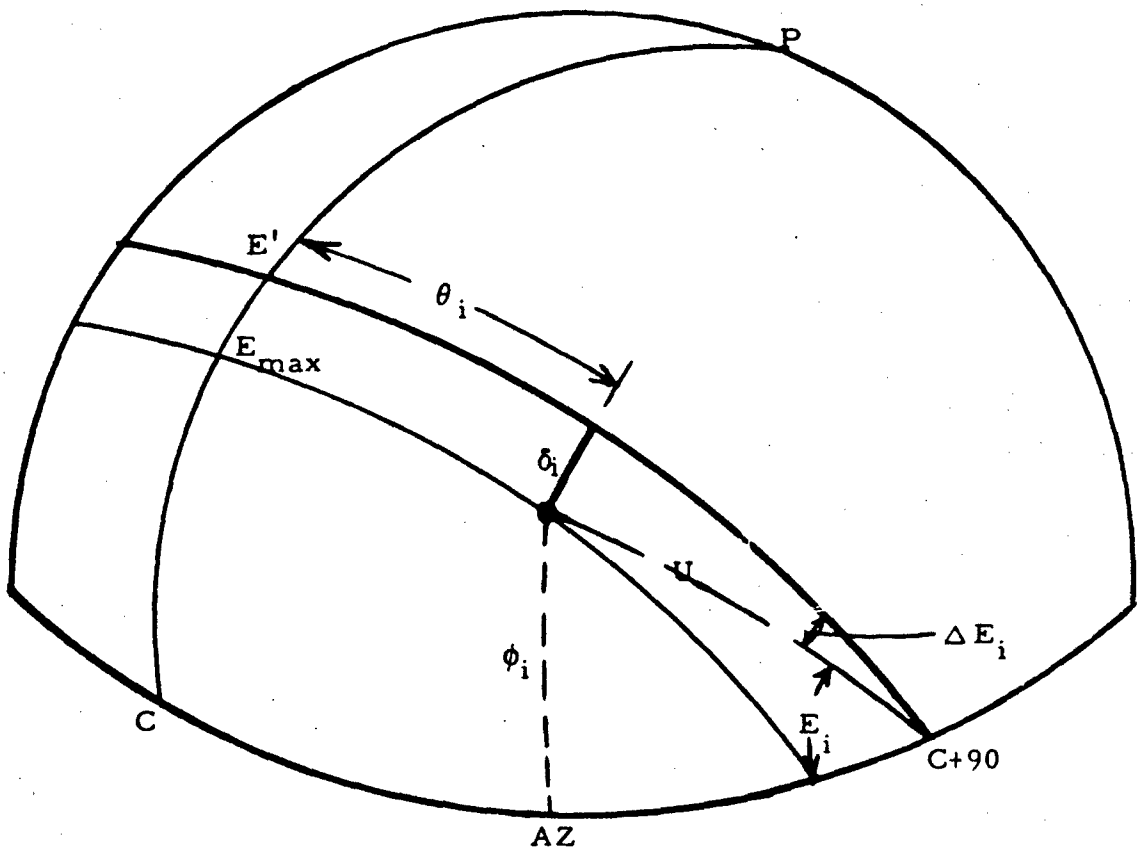

Figure 20

Geometrical relations for calculation of 4-axis parameters by method of Appendix C.

will allow timing of satellite brightness variation to within 1 millisecond, although the present timing system has not been tested on this point, and that the output light curves would display satellite brightness fluctations with frequencies of up to 1 KC. The most rapidly varying satellite yet observed had a tumble period of 0.488 seconds and exhibited four distinct peaks in this interval. The equivalent input frequency of 8 cps is quite low compared with the system capability. Brief transients occuring in only a few milliseconds have been observed from satellites exhibiting specular behavior. One example is the Alouette top-side sounder satellite which exhibits bright flashes from its 75-foot whip antennas.

In its present configuration the photometer will yield measurable records above the system noise for satellites of + 6 to + 7 stellar magnitudes, i.e. at the threshold of naked eye sensitivity. The limitation is incurred by four factors; first, the light-collecting aperture of the optical system; second, the necessity of using field-defining apertures of 4 to 8 minutes of arc for adequate tracking tolerance thus placing the accepted sky background levels at approximately + 8 stellar magnitudes; third, the wide band-width of the photometer system which passes much greater noise power than a conventional stellar photometer and hence imposes a high noise level, and fourth, usage of an uncooled photomultiplier which, while highly suited for high ambient light levels without overload of fatigue, is not the most sensitive tube which could be employed. Of these restrictions the field aperture and lack of cooling of the photomultiplier are the most fundamental.

Tracking is by aided manual track using a bore-sighted guiding telescope of variable power. The operator controls rate of the telescope in the tracking direction and position of the telescope in crosstrack. The operator uses visual position with respect to crosswires and the modulated audio tone as cues in maintaining boresight on the vehicle within his allowed tolerance. Track can be maintained about 75 percent of the time for vehicles at 500 km slant range.

APPENDIX C

The exploratory calculations were not made by solution of the systems of simultaneous equations but by estimating values of the azimuth and zenith distances of culmination, C and Z, by graphical methods and the subsequent calculation of the remaining 4-axis setting parameters by a simpler system of equations. Referring to Figure 20, the following relationships can be established:

FOR E (θ) SYSTEM

Assume E_{max} and C are known. The 3-axis parameters E_i and θ_i are found first, then the 4-axis parameter E'.

$$\tan E_i = \frac{\tan \phi_i}{\cos (Az - C)}$$

$$\sin \theta_i = \cos \phi_i . \sin (Az - C)$$

Estimating the value of δ, ΔE_i is obtained from

$$\sin \Delta E_i = \frac{\sin \delta}{\cos \theta_i}$$

$$E'_i = E_i + \Delta E_i$$

The estimates of δ are repeated until satisfactory constancy of E'_i is obtained. The value of C may require adjustment to avoid asymmetry. (c.f. Figure 12)

FOR δ (θ) SYSTEM

The starting point is again the set of 3-axis coordinates E_i, C, A_{z_i}. Assuming a value for ΔE, the (δ_i, θ_i) are computed from

$$\sin \delta_i = \sin \Delta E . \sin u_i$$

$$\cos \theta_i = \frac{\tan \delta_i}{\tan \Delta E}$$

where the auxiliary angle u is defined by

$$\cos u_i = \cos \phi_i \sin (A_{z_i} - C)$$

Unclassified
Security Classification

DOCUMENT CONTROL DATA · R&D

(Security classification of title, body of abstract and indexing annotation must be entered when the overall report is classified)

1. ORIGINATING ACTIVITY (Corporate author)
General Physics Research Laboratory
Aerospace Research Laboratories
Office of Aerospace Research

2a. REPORT SECURITY CLASSIFICATION
Unclassified

2b. GROUP

3. REPORT TITLE
"Advantages of a 4-Axis Tracking Mount for the Photoelectric Photometry of Space Vehicles"

4. DESCRIPTIVE NOTES (Type of report and inclusive dates)
Scientific Internal

5. AUTHOR(S) (Last name, first name, initial)
Kissell, Kenneth E.

6. REPORT DATE	7a. TOTAL NO. OF PAGES	7b. NO. OF REFS
December 1965	41	15

8a. CONTRACT OR GRANT NO.	9a. ORIGINATOR'S REPORT NUMBER(S)
b. PROJECT NO. 7114	
c. 61445014	9b. OTHER REPORT NO(S) (Any other numbers that may be assigned this report)
d. 681301	ARL 65-260

10. AVAILABILITY/LIMITATION NOTICES
Distribution of this document is unlimited.

11. SUPPLEMENTARY NOTES	12. SPONSORING MILITARY ACTIVITY
	Aerospace Research Laboratories (ARP) Office of Aerospace Research Wright-Patterson AFB, Ohio

13. ABSTRACT

Arguments are presented for the necessity of using a four-axis telescope (Quad-R-Axial) mount for the photoelectric photometry of satellites if small field apertures and hence low sky background signals are to be achieved. Since the signal to noise ratio of the target/ background is proportional to the square of the diameter of accepted field, any reduction of guiding errors which will allow smaller field apertures will then allow the photometry of fainter satellites, providing telescopes of adequate aperture are used. The improved tracking will also reduce interruptions of the light curves resulting from loss of the vehicle from the sensing aperture. The improvements possible with a QRA mount over the 2-axis (alt-azimuth) and the 3-axis (Baker-Nunn) are shown and procedures for computation of mount settings established. Photoelectric data taken with an existing 3-axis system are given for several satellites.

DD FORM 1 JAN 64 1473

Unclassified
Security Classification

Unclassified
Security Classification

14. KEY WORDS	LINK A		LINK B		LINK C	
	ROLE	WT	ROLE	WT	ROLE	WT
1. Satellite 2. Photometry 3. Multi-axis tracking mount 4. Satellite signatures 5. Photoelectric photometry						

INSTRUCTIONS

1. ORIGINATING ACTIVITY: Enter the name and address of the contractor, subcontractor, grantee, Department of Defense activity or other organization *(corporate author)* issuing the report.

2a. REPORT SECURITY CLASSIFICATION: Enter the overall security classification of the report. Indicate whether "Restricted Data" is included. Marking is to be in accordance with appropriate security regulations.

2b. GROUP: Automatic downgrading is specified in DoD Directive 5200.10 and Armed Forces Industrial Manual. Enter the group number. Also, when applicable, show that optional markings have been used for Group 3 and Group 4 as authorized.

3. REPORT TITLE: Enter the complete report title in all capital letters. Titles in all cases should be unclassified. If a meaningful title cannot be selected without classification, show title classification in all capitals in parenthesis immediately following the title.

4. DESCRIPTIVE NOTES: If appropriate, enter the type of report, e.g., interim, progress, summary, annual, or final. Give the inclusive dates when a specific reporting period is covered.

5. AUTHOR(S): Enter the name(s) of author(s) as shown on or in the report. Enter last name, first name, middle initial. If military, show rank and branch of service. The name of the principal author is an absolute minimum requirement.

6. REPORT DATE: Enter the date of the report as day, month, year; or month, year. If more than one date appears on the report, use date of publication.

7a. TOTAL NUMBER OF PAGES: The total page count should follow normal pagination procedures, i.e., enter the number of pages containing information.

7b. NUMBER OF REFERENCES: Enter the total number of references cited in the report.

8a. CONTRACT OR GRANT NUMBER: If appropriate, enter the applicable number of the contract or grant under which the report was written.

8b, 8c, & 8d. PROJECT NUMBER: Enter the appropriate military department identification, such as project number, subproject number, system numbers, task number, etc.

9a. ORIGINATOR'S REPORT NUMBER(S): Enter the official report number by which the document will be identified and controlled by the originating activity. This number must be unique to this report.

9b. OTHER REPORT NUMBER(S): If the report has been assigned any other report numbers *(either by the originator or by the sponsor)*, also enter this number(s).

10. AVAILABILITY/LIMITATION NOTICES: Enter any limitations on further dissemination of the report, other than those imposed by security classification, using standard statements such as:

(1) "Qualified requesters may obtain copies of this report from DDC."

(2) "Foreign announcement and dissemination of this report by DDC is not authorized."

(3) "U. S. Government agencies may obtain copies of this report directly from DDC. Other qualified DDC users shall request through _____."

(4) "U. S. military agencies may obtain copies of this report directly from DDC. Other qualified users shall request through _____."

(5) "All distribution of this report is controlled. Qualified DDC users shall request through _____."

If the report has been furnished to the Office of Technical Services, Department of Commerce, for sale to the public, indicate this fact and enter the price, if known.

11. SUPPLEMENTARY NOTES: Use for additional explanatory notes.

12. SPONSORING MILITARY ACTIVITY: Enter the name of the departmental project office or laboratory sponsoring *(paying for)* the research and development. Include address.

13. ABSTRACT: Enter an abstract giving a brief and factual summary of the document indicative of the report, even though it may also appear elsewhere in the body of the technical report. If additional space is required, a continuation sheet shall be attached.

It is highly desirable that the abstract of classified reports be unclassified. Each paragraph of the abstract shall end with an indication of the military security classification of the information in the paragraph, represented as *(TS), (S), (C), or (U)*

There is no limitation on the length of the abstract. However, the suggested length is from 150 to 225 words.

14. KEY WORDS: Key words are technically meaningful terms or short phrases that characterize a report and may be used as index entries for cataloging the report. Key words must be selected so that no security classification is required. Identifiers, such as equipment model designation, trade name, military project code name, geographic location, may be used as key words but will be followed by an indication of technical context. The assignment of links, rules, and weights is optional.

GPO 886-551

Unclassified
Security Classification